DOCTORAL (Ph.D.) THESIS

Advanced Imaging in Traumatic Brain Injury

Arnold Tóth MD

Doctoral School of Clinical Neurosciences

Clinical and Human Neurosciences Program

Supervisors:

Attila Schwarcz, MD, PhD

Prof. József Janszky, MD, PhD

Program Leader: Prof. József Janszky, MD, PhD

Doctoral School Leader: Prof. Sámuel Komoly, MD, PhD

Department of Neurosurgery, University of Pécs, Medical School

Pécs, 2017

TABLE OF CONTENTS

ABBREVIATIONS

ADC - Apparent diffusion coefficient

BOLD - Blood oxygen level dependent

CSF – Cerebrospinal fluid

DAI - Diffuse axonal injury

DTI - Diffusion tensor imaging

EPI - Echo-planar imaging

FA – Fractional anisotropy

FLAIR - Fluid attenuation inversion recovery

fMRI - Functional MRI

GCS - Glasgow coma scale

ICV – Intracranial volume

LOC – Loss of consciousness

LVR – Lateral ventricle ratio

MD- Mean diffusivity

MPRAGE – Magnetization prepared rapid acquisition gradient echo

mTBI – Mild traumatic brain injury

OR – Odds ratio

PTA - Posttraumatic amnesia

RR – Relative risk

ROC – Receiver operator curve

SD – Standard deviation

sTBI – Severe traumatic brain injury

SWI - Susceptibility weighted imaging

TBI – Traumatic Brain Injury

TBSS – Tract based spatial statistics

TE – Echo time

TI – Inversion time

TR – Repetition time

I. INTRODUCTION

Traumatic brain injury (TBI) constitutes a public health problem worldwide, because of its high incidence, morbidity and mortality. TBI is a leading cause of death and disability in the young, otherwise healthy, employed population that does not only mean a personal, or family-wise disaster, but a social burden as well.

TBI is a very heterogeneous disease and affects the most complex organ of the body. The underlying pathomechanisms are still poorly understood. The present diagnostic tools might only reveal the “tip of the iceberg”, the proper therapeutic methods are equivocal and the protocols largely differ among the TBI centers. Hippocrates is said to have remarked in 400 BC that “No head injury is too severe to despair of, nor too trivial to ignore”. This statement briefly underscores the difficulties regarding the diagnosis and prognosis of TBI. His words are relevant even today.

The aim of the present thesis is to test if advanced neuroimaging can provide better insights into TBI induced alterations, thus aiding TBI diagnosis.

1.1 Definitions and classification of TBI

Traumatic brain injury can be defined as a nondegenerative, noncongenital insult to the brain from an external mechanical force, possibly leading to permanent or temporary impairment of

cognitive, physical, and psychosocial functions, with an associated diminished or altered state of consciousness.

The definition of TBI has not been consistent and tends to vary according to specialties and circumstances. The term brain injury is often used synonymously with head injury, which may not be associated with neurologic deficits. The classification, especially regarding severity, also has been problematic with variations in the inclusion criteria. When reporting studies of TBI, it is therefore beneficial to highlight the inclusion and exclusion criteria that were applied exactly.

- It is possible to classify brain injury as primary and secondary. Primary injury is induced by a mechanical force and occurs at the moment of the injury; the two main mechanisms that cause primary injury are contact (e.g. an object striking the head or the brain striking the inside of the skull) and acceleration-deceleration[1]. Secondary injuries include a very wide array of mechanisms occurring hours to weeks after the primary insult. The most important contributing factors are edema formation, raised intracranial pressure, decreased cerebral blood flow and inflammation-like processes leading to cell death.

- Injuries can be classified as focal and diffuse. Focal injuries include e.g scalp injury, skull fracture and surface contusions that are generally caused by the contact. Diffuse injuries include diffuse axonal injury (DAI), hypoxic-ischemic damage, meningitis, and vascular injury; usually caused by acceleration-deceleration forces.

- A closed (non-missile) head injury occurs when the dura mater remains intact. The skull can be fractured, but not necessarily. A penetrating head injury occurs when an object pierces the skull and breaches the dura mater.

- Brain injuries may be classified upon the mechanism and energy of the injury. High-energy head injuries include: a, Falls in which the head strikes an object with significant force – a fall from a height of 1.2 m (4 ft) may be enough to cause such an injury b, Car crashes in which the head strikes and cracks or breaks the windshield or dents the inside of the vehicle c, Sports injuries, such as striking the head after falling from a fast-moving bicycle d, Direct blows to the head with a hard object, such as a fist or a baseball bat swung with significant force.

- Mechanisms may be grouped as: Object against head, head against object, head against ground, acceleration-deceleration injury (e.g. head against relatively soft material, or head in helmet) and blast related injury.

- Classification can be based on the clinical severity. The most widely used clinical parameters indicating injury severity are the following:

a, Glasgow Coma Scale (GCS): A 3- to 15-point scale used to assess a patient's level of consciousness and neurological function[2] ; scoring is based on best motor response, best verbal response, and eye opening (e.g. eyes open to pain, open to command).

b, Duration of loss of consciousness (LOC): Classified as mild (mental status change or LOC < 30 min), moderate (mental status change or LOC 30 min to 6 hr), or severe (mental status change or LOC >6 hr)

c, Duration of Posttraumatic amnesia (PTA): The time elapsed from injury to the moment when patients can demonstrate continuous memory of what is happening around them.

The most common classification system for TBI severity is based on the Glasgow Coma Scale (GCS) score determined at the first presentation. A total score of 3-8 for the 3 sections indicates severe

TBI (sTBI), a score of 9-12 indicates moderate TBI, and a score of 13-15 indicates mild TBI (mTBI). Generally, sTBI requires a neurointensive care, moderate TBI patients are admitted to a neurosurgical department for long term observation, while an ambulatory presentation with the exclusion of possible complications and a short observation is due for mTBI patients.

Though GCS is still the fastest and most reliable way to assess the level of consciousness, it has significant limitations. Factors most commonly limiting the reliability of GCS are the following: alcohol or drug intoxication, sedation, intubation, psychiatric/mental disease, direct trauma of the eye or face/mouth and peripheral (nerve) injuries[3].

Not surprisingly, most issues with the use of GCS occur in the mid-range (9-13)[4].

The assessment of LOC and PTA might be substantial to better evaluate the brain injury severity in the mild-moderate range. Several severity classification systems and mTBI definitions include also LOC and PTA besides GCS to discriminate between mild and moderate TBI. Of course, the evaluation of both LOC and PTA may be elusive, as their assessment mostly relies on a heteoanamnesis (if available) and are again, biased by non-brain-injury dependent factors such as intoxication or accompanying mental diseases. Some classification systems also include the CT results (see chapter 1.4 - computed tomography).

As a summary, it is important to note that the severity classification of TBI is greatly based on clinical parameters, which, however may be strongly influenced by non-injury related factors, so the actual brain damage extent and type may not be precisely diagnosed. There's a clear need for additional tools such as imaging or biomarker (lab test) methods, not only to identify brain pathologies that require a surgical intervention, but to provide a more accurate diagnosis of the brain injury components and severity.

1.2 Epidemiology of traumatic brain injury

The epidemiology of TBI has been most extensively studied in the USA. According to these studies, approximately 2.5 million TBI-related emergency department visits, hospitalizations, or deaths occur in the United States annually. The following annual statistics from the Centers for Disease Control and Prevention also apply to the United States[5]: TBI contributes to approximately 50,000 deaths. Approximately 475,000 TBIs occur among infants, children, and adolescents aged 0-14 years. About 80,000-90,000 people experience the onset of a long-term disability due to a TBI.

The following groups are at particular risk for TBI: males are about twice as likely as females to sustain a TBI, infants and children aged 0-4 and adolescents aged 15-19 years are the 2 age groups at highest risk for a TBI, adults aged 75 years or older have the highest rates of TBI-related hospitalization and death.

The leading causes of TBI are as follows: Falls (28%), motor vehicle crashes (20%), being struck by or against objects (19%) and assaults (11%).

Mortality rates after brain injury are the highest in people with a sTBI. In the first year after a TBI, people who survive are more likely to die from seizures, septicemia, pneumonia, digestive conditions, and all external causes of injury than are other people of similar age, sex, and race[6]. However, the mortality rate after sTBI has decreased since the late 20th century[7].

According to the Centers for Disease Control and Prevention, the economic cost of TBI in the United States in 2010, including direct and indirect medical costs, was estimated at $76.5 billion.

The incidence of TBI in Hungary is estimated to be around 200/100.000. Approximately 80% of the cases are mild, and less than 10% are severe. However, mTBI appears to be vastly underdiagnosed in the setting of systemic trauma, even in trauma centers [8]. Unfortunately, the mortality rate of sTBI in Hungary almost reaches 50%[9].

1.3 Diffuse axonal injury (DAI)

Diffuse axonal injury is one of the most important pathological components of TBI, as a result of traumatic acceleration/deceleration or rotational shear-strain forces leading to axonal/myelin stretching or disruption[10, 11]. Previously, DAI has been considered a primary-type injury, with the damage occurring at the time of the accident. Research has shown that another component of the injury comprises the secondary factors (or delayed component), since the axons are injured, secondary swelling occurs, and retraction bulbs form leading to complete disconnection[12]. Originally DAI was suggested upon an inferential basis, in any patient who demonstrated clinical symptoms disproportionate to his or her CT-scan findings, and was generally restricted for comatose patients, whose vast majority (>90%) remained in a persistent vegetative state. Recently, however the term DAI (or the synonym traumatic axonal injury) has been more widely used, applying to the entire severity range of TBI, including a spectrum of axonal damage from a subtle, reversible functional disorder to the true disconnection[13].

The extent and severity of DAI is highly related to the clinical severity and outcome[13]. However, clinical diagnostic tools including imaging fail to detect DAI due to its microscopic range. One

possible target in order to provide better diagnosis and prognosis for advanced imaging methods is DAI (see chapter 1.5).

1.4. Conventional imaging in traumatic brain injury

The gold standard imaging method in acute TBI is the non-enhanced head CT scan[14, 15]. Performing a plain head x-ray makes no sense due to its low sensitivity and specificity to trauma-related pathologies. CT scan plays a substantial role in the detection of pathologies that require a surgical intervention, also in the follow-up and in the assessment of the prognosis. Though conventional MRI has been shown to be somewhat more sensitive to small focal traumatic lesions, its clinical value is not clear yet. Performing conventional MRI in TBI may be though advantageous in the sub-acute phase of TBI (2-3+ days after the injury), when bleeding may become isodense in CT scans but becomes well identifiable on MR scans.

Computed Tomography (CT)

Computed tomography is the gold standard imaging choice in TBI. The advantage of CT scanning is that it is readily available in every trauma center and even agitated patients can be examined due to the short acquisition time. It provides voxelwise X-ray attenuation maps with good spatial resolution and acute haematomas can be easily visualized due to their high degree of X-ray attenuation.

The disadvantage of the technique is that it applies ionization radiation thus it may add a risk to cancer development – a problem significantly reduced in novel low radiation instruments. Other disadvantage is that diffuse white matter lesions mostly remain hidden on the images.

The main purpose of CT scanning is the identification of those patients who need hospitalization and further observation and surgical intervention. It should be noted that only a minority of patients (< 10%) with inclusion criteria for mTBI will have a positive CT scan[14, 16, 17].

The question is when or when not to perform a head CT. Several guidelines[18, 19] have been put forward to determine the circumstances when CT scanning is required. Probably the most widely used CT indication system are the Canadian head CT rule[20] and The New Orleans guide[14]. Common points for indication of a CT in patients with mTBI are the following: LOC, vomiting, amnesia, suspected cranial fracture (basal, open, or depressed), neurological deficit, coagulopathy, post traumatic seizure, age > 60y, high energy injury (i.e. fall from height, motor vehicle accident etc.)

By several definitions, TBI is considered “mild” when the CT is negative, and due to the majority of classifications, is considered “complicated mTBI”, or “moderate” TBI when any pathology can be identified. In suspected mTBI CT may visualize small macroscopic hemorrhages such as cerebral contusions, traumatic subarachnoidal hemorrhages, extra-, or subdural hematomas. Nevertheless, small hematomas in patients with mTBI may remain hidden due to the partial volume effect (mostly on the bone-brain interface) on the temporal and frontal skull bases. Such hemorrhages in mTBI appear to progress within the first 2h after injury and reach their final volume within 24h[21]. It is of note that acute CT pathologies in mTBI may not predict the outcome 3 months after injury[22], and clinical variables together with age may be stronger predictors for

long term outcome[23]. DAI is basically invisible in CT, punctual hyperdensities in the white matter, as signs of microbleeds accompany DAI only very rarely.

The above listed limitations of CT in terms of resolution and/or outcome prediction ignited the search for advanced neuroimaging modalities in mTBI.

The need of a CT in moderate and sTBI is not questionable. In these severity groups, the occurrence of pathologies needing follow-up or intervention that can be detected by CT is very high. Beyond its significance in the clinical management, unlike in mTBI, in moderate and sTBI, CT plays an important role in setting up the prognosis. As mentioned before, clinical parameters as GCS, alone have limited prognostic power. Countless CT signs and alterations have been tested for their prognostic value[24]. Not surprisingly, it turned out that some CT signs provide a better prognostic value in combination than alone, efforts have been done to sort and weigh the most important CT signs to create prognostic systems. The first such TBI CT classification and prognostic system was the Marshall score[25], see **Table 1.4.1**. This system has been widely used and validated[26].

Table 1.4.1

Modified Marshall CT grade

I	Diffuse injury	No visible pathology	1
II	Diffuse injury (With present cisterns, midline shift 0-5mm and/or small (< 25cc) high or mixed density lesions)	No lesions	2a
		Only one lesion	2b
		>1 unilateral lesion	2c
		Bilateral lesions	2d
III	Diffuse injury and swelling	I-II + compressed or absent cisterns	3
IV	Diffuse injury and shift	I-III + >5mm midline shift	4
V	Evacuated mass lesion(s)	Extradural	5a
		Subdural	5b
		Intracerebral	5c
		>1 intra + extracerebral	5d
VI	Non-evacuated mass lesion (>25cc)	Extradural	6a
		Subdural	6b
		Intracerebral	6c
		>1 intra + extracerebral	6d

Later, Maas et al. tested the prognostic value of individual CT signs, such as midline shift, basal cistern compression, intraventricular bleeding and traumatic subarachnoid bleeding. They investigated if these, or a different distribution of the included signs might improve the Marshall score. The addition of subarachnoid and intraventricular bleeding, and the further differentiation of basal cistern compression, midline shift and mass bleeding brought a better prognostic effect. This system is referred to as the Rotterdam score[27] (see **Table 1.4.2.**), and has been shown to be a better prognostic tool than the Marshall score[28, 29].

Table 1.4.2.

Rotterdam CT classification

Predictor	Score
Basal cisterns	
Normal	0
Compressed	1
Absent	2
Midline shift	
No shift or shift ≤ 5 mm	0
Shift > 5 mm	1
Epidural mass lesion	
Absent	0
Present	1
Intraventricular blood or subarachnoid hemorrhage	
Absent	0
Present	1
SUM score	+1

It can be noted, that midline shift and cistern compression is an important factor in both systems, so one might conclude that bleedings or edema with a mass effect may be one of the most frightening CT signs in TBI. The present score systems are based on largely subjective, conventional CT scan reading. Research has focused on the possibility of enhancing the prognostic value of CT in TBI when adapting quantitative image analysis for the aforementioned CT signs, see chapter 1.5 - Quantitative CT in severe traumatic brain injury.

Prognostic power can be dramatically increased when clinical parameters are combined with CT signs. Based on the investigation of several-thousand patients, the most important clinical and CT parameters with the best weighting factor were described and included in the IMPACT prognostic model[30, 31]. This model is freely available online (http://www.tbi-impact.org/?p=impact/calc), and was externally validated[31]. These prognostic systems can be

used to predict 6-month mortality or unfavorable outcome, i.e. vegetative state or severe disability.

Conventional MRI

Conventional MRI (T1-, T2-, proton density weighted, Fluid Attenuation Recovery -FLAIR) generally depicts traumatic alterations, especially the focal ones in a more detailed fashion than CT[32-34]. MRI makes the evaluation of the brainstem, the subcortical gray matter and the cerebellum easier. Generally, MRI reveals 10-30% more abnormalities than CT, the difference is more pronounced in the less severe cases. However, in many cases of TBI, conventional MRI also fails to detect the diffuse and subtle damage[35, 36], and the clinical interpretation of the detected lesions is debatable[37]. The high expenses, low availability, relative and absolute contraindications of MRI also significantly limit the role of MRI in acute TBI.

Although CT remains the gold standard imaging modality for acute TBI, MRI is recommended in children and young women due to the absence of ionizing radiation. MRI may be superior to CT 48 hours after the injury, when bleeding may become isodense on CT scans but becomes well identifiable on MR scans. Moreover, based on the altered magnetic properties of hemoglobin degradation, MRI is able to precisely define the time of bleeding onset, i.e. is able to clearly depict a series of re-bleeding that makes MRI an excellent tool for follow-up[38, 39].

However, the main interest regarding the use of MRI in TBI aims the advanced MRI methods, which may be able to sensitively reveal traumatic microstructural and functional abnormalities, see next chapter.

1.5 Advanced imaging in traumatic brain injury

Here we define advanced imaging as quantitative modalities and/or post processing methods that are available in research, but yet have not been widely applied in clinical environments. In the field of mTBI, advanced imaging mainly means advanced MRI methods, as diffusion tensor imaging (DTI), functional MRI (fMRI), volumetric analysis and susceptibility weighted imaging (SWI) that offer very sensitive microstructural and functional mapping of TBI. Though a large set of studies have conducted advanced MRI investigations in sTBI as well, their feasibility in sTBI is clearly limited, not merely because of the issues related to patient management (anesthesia, MRI safety issues), but also because the major pathologies such as bleedings, fractures and distorsions constitute MRI artifacts and post-processing challenges.

In sTBI, advanced imaging offering novel insights into diagnosis and prognosis assessment mainly involves quantitative CT analysis. Presently the CT signs are assessed qualitatively, quantitative evaluation (e.g. midline shift) is restricted to the use of linear (1 dimensional) measurements. Semi-automated 3-dimensonal, volumetric based assessment might enhance the evaluation of traumatic CT signs.

The need for advanced MRI in mild traumatic brain injury

Mild TBI is a special field calling for advanced imaging, first of all MRI methods. The numerous different definitions for mTBI and inconsistent terminology (e.g concussion, minor head injury, minor brain injury, minor head trauma etc.) show that the confinement of this clinical category

is pretty challenging. Diagnosis is mostly based on symptoms and self-reported history, yet no generally deployable objective marker exists, however recent attempts for both imaging- and biomarkers are promising. The most widely accepted criteria for mTBI are the following: blunt trauma, Glasgow Coma Scale (GCS) of 13-15, brief period (< 30 min) of LOC, brief period (< 24h) of post traumatic amnesia[40, 41]. Inclusion of cases where CT scans show trauma related pathology is debated, mostly these cases are excluded i.e. mTBI is considered to be CT scan negative. Indeed, CT scans are normal in around 90% of the cases fulfilling the aforementioned criteria. This is paradoxical considering the sometimes alarming neuropsychological signs and symptoms of these patients. In these cases, probably the major part of the damage, which is related to a certain degree of axonal = microstructural disintegration, is hidden on the CT scans. The categorization of CT positive mTBI cases as "complicated mTBI" (e.g. finding of focal contusion) seems to be useful because these cases generally deserve extra attention acutely. Focal lesions, however may not predict the outcome 3 months after injury[22], clinical variables together with age may be stronger predictors[23].

Beyond the issues with definitions and diagnostic criteria the greater problem from a clinical point of view is that signs and symptoms at admission are only very scarcely linked to the prognosis and true severity of the injury. This means that e.g. LOC or the length of PTA is not necessarily associated with the actual mechanical force suffered or the chance of developing persistent posttraumatic complaints. It's important to keep in mind that mTBI can be interpreted as "mild" only when compared to moderate or sTBI known to be life-threatening. In itself, mTBI is also potentially dangerous as in 10-30% of the cases it may lead to serious long term complications significantly worsening life quality and also disabling work or social interactions[42,

[43]. Additionally, considering its extremely high incidence (up to 500/100.000) mTBI also deserves to be called a public health problem. Long term complications may include long persisting acute symptoms, as headache, dizziness, nausea, concentration/memory problems though new complaints may also develop by time such as depression, sleeping disorders, or anxiety[44, 45]. Patients suffering from repetitive mTBI, or even from repetitive sub-concussions are especially exposed to long term complications[46]. This makes the decision on letting one back to work, or return to play (in case of sports concussion) truly responsible[47]. Still, without enough objective information on mTBI related mechanisms, the background of long term complications is not fully understood. It is debated, if they are a result of psychological or organic factors.

Until mTBI related pathomechanism remains elusive, therapeutic possibilities are also going to be limited. Presently the only widely accepted treatment is rest, both physical and cognitive. Medications used serve merely symptomatic treatment and their use is generally based on local anecdotal evidence[48].

One reason why identification of the details of related mechanisms is delayed is that generally histopathological examination is of course not possible. Human histopathological observations are very scarce, from the rare cases when mTBI was accompanying fatal conditions by chance[49]. The vast majority of histological information and data about pathomechanism of mTBI has been therefore obtained from animal (mostly rodent) models (for an overview see [50]). These models allow an infinite range of controlled observations on different elements of brain injury, and have provided irreplaceable findings so far. However all mTBI animal models suffer from the problem that mTBI can only be interpreted truthfully at the complexity of the human brain. Most of the signs and symptoms characterizing this condition are hardly transposable to animals, such as

cognitive disorders, headache, dizziness, depression. To be simplistic, mTBI is grossly the damage of a higher order fraction of the human brain that an animal does not even have.

The aforementioned concerns regarding mTBI diagnosis, prognosis evaluation and pathomechanism have together called for the non-invasive, highly sensitive contemporary imaging tools. Among single photon emission computed tomography (SPECT), positron emission tomography (PET) and MRI, the latter has become the most widely applied in mTBI studies because it's the most accessible, multimodal and is the least harmful since no ionizing radiation is used and generally no contrast agent has to be administered either. Multimodality in MRI means that this method, depending on actual acquisition parameters, can provide different insights to the complex pathology of the damaged brain, from detailed microstructural to functional components. Unlike classic neuroradiological scan evaluation, assessment of advanced MRI data are often based on quantitative and statistical methods. This means that though visible images are created here as well, the true information is held in the underlying numbers allowing objective, often group-wise analyses.

One of the most promising methods in the field is diffusion tensor imaging (DTI) that is able to detect change in water micro-compartments due to microstructural pathology such as axonal deformation and swelling. Focal microscopic bleeds developing as part of DAI are most successfully detectable by susceptibility weighted imaging (SWI), a method exploiting the magnetic property of iron. High resolution, three-dimensional T1 weighted images allow precise volumetric analyses to be performed shedding light on subtle changes in the brain macrostructure, due to e.g. edematic and atrophic mechanisms following injury. Getting to

functional level, the effect of injury on brain functions as perception or also cognitive tasks (as typically affected memory and concentration functions) can be investigated fMRI.

Diffusion Tensor Imaging (DTI)

DTI measures Brownian movement of water molecules and applies at least six diffusion gradient directions, thus is able to provide information on both the extent and directionality of diffusion[51]. Fractional anisotropy (FA) refers to the degree of directionality, calculated from the ratio of eigenvalues of the diffusion tensor, while mean diffusivity (MD) or the synonym apparent diffusion coefficient (ADC) refers to the overall, directionally indifferent mobility of water molecules. Diffusivity character in the brain is widely accepted to be associated with the fiber tracts i.e. axons and myelin sheath[52]. According to the classic theory, in the direction parallel to axons diffusion is greater than perpendicular, since cell membranes and other structures restrict diffusion. This is why white matter tracts can be visualized by DTI tractography. Though this concept has never been exactly confirmed, tremendous empirical data shows that it works quite well. FA and MD are very sensitive parameters indicating subtle alterations of white matter because they are influenced by the axon density, -diameter, -continuity, myelin content, myelin sheath thickness and interstitial water content. This way DTI can reveal individual differences among healthy subjects as well, for example gender, age or education level are known to have an effect on DTI parameters.

Therefore, it's not surprising that DTI is able to detect axonal pathology in sTBI, however it might be surprising that up till now it can be regarded as a fact that DTI finds white matter abnormalities

in mTBI as well. These abnormalities include axonal disintegration related to shear-strain deformation of the fiber structure, basically a mild form of DAI. Changes in water micro-compartments because of vasogen or cytotoxic edema may also be present, and are detectable with DTI[53].

A large cohort of studies investigated diffusion in mTBI focusing on several different relations, e.g. with age, acute or chronic phase, clinical symptoms or neuropsychological tests, recovery, sport- and combat related injuries[54].

Findings of follow-up studies are also various. Some longitudinal studies revealed partial normalization of DTI indices after different periods [55-57], while other investigations indicated traumatic microstructural alteration to be more permanent[58] or even to evolve over time[59]. There are promising observations about the relation of DTI findings with cognitive or psychological dysfunction[60, 61] and clinical outcome[62], especially in moderate to severe cases[57, 63].

Beside temporal features of white matter changes, spatial characteristics also imply several questions. Though axonal pathology is regarded mostly diffuse in mTBI, it's clear that some regions must be more vulnerable due to general mechanical and anatomical rules even if considering subject variability. For instance, posterior corpus callosum seems to be the most susceptible to mild injuries[64]. In some cases, injury of a certain white matter tract is obviously associated with the accompanying complaint. In other situations the complaint can rather be linked to the extent of overall injury. Based on clinical history only, it's impossible to exactly draw the model of biomechanical forces and thus predict the predominant site (fascicle) of injury, though some attempts can be performed on e.g. sports concussion cases where video recordings of the incident are available and can be analyzed by specialized computer algorithms. DTI offers

retrospective assessment of the manifestation peak sites of axonal injury that can be correlated with occurring signs and symptoms. For example in case of damage of tracts originating from hippocampal areas impaired memory functions may be more easily understood. If imaging is performed in the chronic phase, it's challenging to decide if DTI abnormalities then are a cause or a result of the clinical disorders, since mTBI independent disorders (as e.g. depression) themselves may also be associated with DTI abnormalities[65]. The specificity of posttraumatic neuropsychological testing for DTI results in mTBI is a topic of debate as well, since non-TBI factors may affect both[66].

Though several aspects of DTI in TBI has been revealed, it's unclear if DTI is still able to detect alteration in very mTBI (GCS = 15, minor LOC, CT and conventional MRI normal). The literature is scarce on understanding the acute dynamics of DTI parameters, the aforementioned different (opposite) parameter findings may be explained by the different timing of the acquisitions. If image acquisition timing affects DTI parameters after the injury, DTI dynamics should be profoundly known to draw the proper conclusions from the findings.

Susceptibility weighted imaging (SWI)

Susceptibility weighted imaging is particularly sensitive in detecting both intravascular venous deoxygenated blood and extravascular blood products[67, 68]. This method exploits the magnetic property of heme iron. Iron causes local magnetic field distortion altering both T2 star relaxation times and phase data that are measurable and can be visualized by proper MRI sequence (high resolution fully velocity-compensated T2* 3D gradient echo). Anatomical structures do not

appear well on these images, contrast is low between e.g. cortex and white matter or cerebrospinal fluid (CSF), in turn iron content, most importantly bleeding is shown pronouncedly in form of hypointense (black) lesions.

SWI was shown to be the most sensitive MRI modality for detecting micro hemorrhages, primarily in pediatric TBI of mixed severity[69, 70]. SWI does not only reveal more focal lesions in a certain patient than other MRI modalities such as T2 weighted imaging, FLAIR, gradient recalled echo or CT does, but SWI hemorrhagic lesions are also less likely to be overlooked. This is supported by inter-rater-reliability data[71].

It was possible to explore correlation of SWI lesion number, volume and location with neuropsychological functioning[69] or with outcome[70] in children. A pediatric patient can be reliably placed in the spectrum of mild- to sTBI based on SWI, with a better prediction of cognitive outcome[72].

In contrast, adult data and especially studies focusing strictly on mTBI are limited. A study proved the superiority of SWI over CT or conventional MRI in sensitivity to microhemorrhage in a group of adults including dominantly sTBI patients[73].

Microhemorrhages do not seem to be that frequent in mTBI. Based on a study of amateur and professional boxers[74], and on experiences of SWI using diagnostic centers, SWI lesions in mTBI occur in about one or two out of ten patients. Thus, large cohorts are needed to make correlations with clinical parameters possible. An attempt toward this was successfully done by Yuh EL et al. who found that hemorrhagic lesion number of four detected early after injury can be regarded as a threshold in predicting a poorer three month outcome[75].

Based on SWI findings, it has been proposed to classify mTBI as hemorrhagic and non-hemorrhagic[76]. The clinical importance of this classification still needs to be addressed.

Volumetric analysis

Brain volume changes like edema and chronically developing atrophy are long while known mechanisms in sTBI. These dramatic volume disorders can be well evaluated by classical manual morphometric measurements. Different manifestations of brain atrophy following injury were identified in a large number of morphometric studies conducted on mixed (mainly moderate to severe) TBI populations[65-67, 77]; Injury severity or cognitive function was correlated with atrophy rate[78, 79]. In one group outcome the was found to be independent from atrophy[58]. Some studies presented the association of post-traumatic stress disorder with atrophy of whole brain[80], corpus callosum[81], anterior cingulum[82] and hippocampus[83].

However in mTBI the volume changes are not that apparent, i.e. if present at all, they are too subtle for routine neuroradiology methods to detect them, hence far less data are available. Furthermore, an important point is that in case of comparing two healthy subjects' brain volumes even when normalizing for total intracranial volumes (ICV) we can find great differences between structure volumes. For instance if we compare the normalized ventricular volume of two healthy subjects of same age, gender, education, two-fold or even bigger difference can be found. Hence it's clear that detecting a volume change of a few percent and regarding it trustworthily as a consequence of mTBI is quite problematic. For such investigations, structural images of the highest possible resolution are needed beside proper quantitative-automatic volumetric analysis

algorithms and high-enough subject number. Follow up arrangement is also advantageous[84]. Among the yet few volumetric studies focusing on homogenous mTBI groups, MacKenzie et al. found global atrophy developing in 3 months in a group of mild and moderate injured patients that was correlated with LOC[85]. The presence of atrophy in mTBI was supported by others as well[86]. Gray matter atrophy was detected years after injury by Cohen et al. in a mTBI group[87]. Messe et al. showed decreased gray matter volume, but this was not predictive for outcome[62]. Though group-wise studies providing valuable data of mTBI volumetric changes are growing, yet the single time point volumetric assessment at subject level is not informative enough in mTBI. However, follow-up volumetric analysis was shown to possibly be beneficial in single cases as well[80].

Functional MRI (fMRI)

Functional MRI detects local hemodynamic changes following increased metabolic rate in neural activity, by measuring the blood oxygen level dependent (BOLD) contrast[81, 88].

Specific cognitive, motor, memory tasks or sensory stimulation are repeated and the associated BOLD signals are recorded[89]. Investigation of functional connectivity reveals brain areas with correlated fluctuations (i.e. coupled functionality) during an experimental task or resting state (in the absence of any active task or external stimulus)[82].

Cognitive disorders such as impaired processing speed, concentration and memory problems are typical in mTBI. Functional MRI is hence a plausible tool in mTBI to better understand underlying neural function abnormalities and plasticity, or to detect specific mTBI related functional

patterns[83]. An outstanding advance of fMRI is the opportunity of measuring actual task performance of a patient simultaneously with functional imaging. For example, during a memory task, the number of correct answers or reaction speed can be quantified. This helps the observer interpret the findings, e.g. additional activations in an injured patient performing just as good as a control subject are indicating compensational neural recruitment.

Most studies concentrated on memory functions, especially working memory[90-95]. The altered activation of primarily the dorsolateral prefrontal cortex was suggested to underlie working memory dysfunctions. A few studies focused on declarative/episodic memory[96-98]. In these studies, various injury related changes of BOLD signal level and distribution were detected. Some investigators found attenuated activation in mTBI patients compared to healthy individuals that may be a result of injured neural networks[92, 93, 99, 100]. Others reported increased or additional activation, i.e. involvement of new, normally silent areas[90, 94, 96]. Latter findings are generally explained to be an effect of neural reorganization or functional accommodation. The discrepancy across these findings of hypo- and hyperactivation patterns in mTBI memory tasks was somewhat solved by a recent study pointing out the significance of a working memory task being a continuous or a discrete task[101].

Correlations between BOLD signal change and neuropsychological findings or task performance were proposed by some studies[94, 98, 99], however the alteration of BOLD signal distribution was observed independent of clinical complaints or performance as well[90, 96]. Because fMRI can reveal abnormal brain activity beside normal behavioral performance of the patients, it was suggested to be a more sensitive tool for neuropsychological evaluation than classical tests are[102]. A

relatively low number of longitudinal studies showed the cessation of symptoms over time to be associated with the normalization of cortical patterns[99, 103].

The recent wave of resting state fMRI studies on mTBI patients provided further important insights to the functionality of the injured brain. In this method, the brain's intrinsic connections (functional connectivity) are mapped by the analysis of low frequency fluctuations. An important network of the resting (or deactivation) state of the brain is called default mode network. Default mode network involves brain areas as medial prefrontal cortex, parietal and retrosplenial areas[32]. The extent of these areas and their connectivity strength may get altered due to injury. Depending on the explored areas, both decreased and increased connectivity were registered[104-107]. Alterations in the default mode network connectivity were suggested to be predictive for not only the acute neuropsychological complaints[104, 107], but for the later developing post-concussion syndrome as well[33].

Abnormal functional patterns in mTBI can be interpreted both as cause or consequence of neuropsychological malfunction. This takes the question to a near philosophical question. If certain cortical areas or linked axonal pathways are injured and cause complaints, those may appear as altered function. It is also possible that injury causes a more general and complex abnormality and a certain local BOLD signal alteration is only a mark of that. Integration of structural and functional connectivity data may be a subsequent step to elucidate these dilemmas[108].

Because of the inherent heterogeneity of mTBI, an effort has to be made to study larger and more characterized cohorts by means of injury type, age, psychosocial factors, image acquisition timing following injury.

Quantitative CT in severe traumatic brain injury

The present sTBI CT evaluation protocols are mainly based on the subjective reading of the images resulting in qualitative findings regarding the presence or the absence of certain pathologies. An exclusion is the assessment of the midline shift, for which a linear measurement is applied, i.e. the distance between the septum pellucidum and the theoretical midline (a line connecting the anterior and posterior internal protuberances) of the brain is measured at the level of the interventricular foramina. Rough volumetric estimation of the mixed or high density lesions, to describe if the lesion is over or under 25ccm, may be used to define grades 4 and 6 in the Marshall score. However, in these cases not the actual extent of the pathology (actual size of midline shift in millimeters, or actual size of lesion) is used for further analysis or prognosis assessment, but the "binary output" referring again to the presence or absence of the pathology. One may address the question, if quantification of the pathologies such as cistern compression rate, lesion volume, actual midline shift, bleeding volume etc. might further increase the prognostic value of the CT scans. The literature upon this question is surprisingly scarce. A number of studies proposed linear measurements[28, 109, 110] that are simple enough to be performed in a clinical set as well, however, results from these approaches did not conclusively overcome the conventional CT reading. A reason for this supposedly is that linear measurements are very biased by slice plane and orientation and so might not be sensitive enough to carry extra information. Two-dimensional (area) measurements are affected by the same issue. One way to avoid this problem is to perform three-dimensional, multi-slice measurements. This can be

performed by manual, semi-automated and fully automated techniques, but neither can be widely applied for clinical purposes yet because of their time or software dependence. However, from a scientific point of view, these techniques might be of interest, since they can shed light to alterations and correlations that are not obvious for the bare eye. Through this, pathomechanisms might be better understood. A study applying quantitative analysis has shown that predictive CT markers are largely inter-related, and their importance may be linked to their status as surrogate measures of a more fundamental underlying clinical feature, such as the severity of intracranial mass effect[111]. This study also has shown that the quantitative markers might improve outcome prediction. Yet understanding the temporal features of CT sign inter-relations is necessary.

II. AIMS

The aim of the present thesis is to test if advanced neuroimaging can provide better insights into TBI induced alterations, thus aiding TBI diagnosis.

Advanced MRI techniques were applied in mTBI patients where conventional imaging completely fails to detect any pathology. Quantitative CT was applied in sTBI patients for whom MRI is often not applicable because of practical factors, however objective parameters might provide important additional information that may be missed during conventional CT reading.

Specific aims:

1. To clarify if advanced MRI such as DTI, volumetric analysis, fMRI, SWI are able to detect any brain alterations in the acute to subacute phase after injury in mTBI patients with completely negative CT and routine MRI (T1W, T2W, FLAIR) scans (=”uncomplicated mTBI” patients).

2. To develop a quantitative assessment method of lateral ventricle asymmetry and test if lateral ventricle volume asymmetry might precede midline shift and so might be an early prognostic marker.

III. ADVANCED MRI IN MILD TRAUMATIC BRAIN INJURY

3.1 Subjects and methods

Subjects

Fourteen patients (five females) from the outpatient unit of the department of Neurosurgery with history of mTBI participated in this study. Patients fulfilled the criteria of "uncomplicated" mTBI[112]. Patients had a Glasgow Coma Scale of 15, LOC for less than one minute, PTA for less than 30 minutes (based on the Galveston Orientation and Amnesia Test[113]) and negative posttraumatic CT. Exclusion criteria consisted of history of a neurological or psychiatric disease, alcohol abuse, substance dependence, an earlier TBI and MR incompatibility. All patients were right-handed according to the Edinburgh Handedness Inventory [114]. A control group of 14 age- and sex-matched healthy volunteers following the same exclusion criteria were also involved in the study. All subjects gave a written informed consent under a protocol approved by the local ethical committee. Demographic characteristics of patient and control groups are shown on **Table 3.1.1.**

Table 3.1.1.

Demographic characteristics of patient and control groups

Data	Patients (n = 14)	Controls (n = 14)	(p)
Age (y)			
Men	34,3 ± 19,4 (20-72)	35 ± 19,6 (20-71)	0,94
Women	36 ± 18,6 (21-61)	37,2 ± 18,6 (21-58)	0,92
Total	34,9 ± 18,4 (20-72)	35,8 ± 18,5 (20-71)	0,90
No. of women	5	5	1
Education (y)	13,4 ± 2,2	13,8 ± 2,5	0,69
Right handedness	14	14	1

Data are mean; ± standard deviation; numbers in parentheses are the ranges

Image acquisition

Initial MRI data of patients were acquired within 72 hours after injury (mean: ~2 days, ranging from 12 h to 72 h, referred to as 72h). The second acquisition was performed approximately one month later (mean: 35 days ranging from 28 days to 43 days after injury, referred to as one month). The control group also underwent the two time point acquisition with a similar time frame (average 30 days difference ranging from 27 to 36).

Magnetic resonance imaging was carried out on a Siemens Magnetom TIM Trio 3 Tesla scanner (Enlargen, Germany) with a 12 channel standard head coil. The sequences consisted of high resolution T1-weighted scan (MPRAGE) for volumetric analysis, T2-weighted scan, DTI and SWI which were applied on all subjects. After the localizer scanning for proper orientation, shimming was carried out to maximize field homogeneity.

Anatomical imaging: T1-weighted high resolution images were obtained using a three-dimensional (3D) MPRAGE sequence (TR / TI / TE = 1900 / 900 / 3.41 ms; Flip Angle = 9°; 160 axial

slices; slice thickness = 0.94 mm; no interslice gap; FOV = 210 x 240 mm^2; matrix size = 224 x 256; receiver bandwidth = 180 Hz/pixel).

T2 weighted images were acquired using a turbo spin echo sequence (TR / TE = 6000 / 93ms; Flip Angle = 120°; 30 sagittal slices; slice thickness = 4 mm; no interslice gap; FOV = 193 x 220 mm^2; matrix size = 280 x 320; receiver bandwidth = 220 Hz/pixel.

DTI: DTI was performed using a 2D single-shot diffusion-weighted, spin-echo, echo-planar imaging (EPI) sequence. Diffusion tensor imaging was achieved using twenty optimum non-collinear encoding directions with a diffusion weighting of b = 700 s/mm^2 and a single volume was collected with no diffusion gradients applied. (TR / TE = 8500 / 90 ms; 60 axial slices, slice thickness = 2 mm; FOV = 208 × 256mm^2; matrix size = 208 × 256; receiver bandwidth = 1563 Hz/pixel; 4 averages. The total acquisition time was 12 minutes.)

Advanced shimming was performed prior to the DTI acquisition to optimize the homogeneity of the magnetic field across the brain and to minimize EPI distortions.

SWI: 3D gradient echo SWI sequence was run with following parameters: (TR / TE = 27 / 20 ms; 72 axial slices; slice thickness = 1.5 mm; flip angle = 15; matrix size = 182 x 256; FOV = 173 x 230 mm^2; receiver bandwidth = 120 Hz/pixel).

fMRI: A subset of the subjects (10 patients and 10 control subjects) also underwent fMRI at both time points using the following data acquisition and tasks:

Functional imaging was carried out using 2D single-shot spin echo echo-planar imaging (EPI) sequence with the following parameters during

(1) hometown walking task: TR / TE = 3000 / 36 ms; Flip Angle = 83°; axial slice plane was adjusted to the plane of hippocampus relying on T2 images; 27 slices; slice thickness = 3 mm; no interslice gap; FOV = 200 x 200 mm; matrix size = 128 x 128; receiver bandwith = 1185 Hz/pixel

(2) covert word generation task: : TR / TE = 2000 / 36 ms; Flip Angle =76°; 23 axial slices; slice thickness = 4 mm; no interslice gap; FOV = 210 x 210mm^2; matrix size = 92 x 92; receiver bandwidth = 1360 Hz/pixel

Interleaved slice order was applied to avoid crosstalk between contiguous slices. A total of 165 volumes were acquired during the hometown walking task and 210 volumes during the covert word generation.

Subjects were positioned supine in the scanner. Foam cushioning was used to immobilize the head within the coil to minimize motion degradation. The process of MRI examination and the task paradigms were explained in details previous to the image acquisition.

Hometown walking task paradigm

To evaluate declarative memory retrieval, Roland's hometown walking task[115] was adopted for fMRI similarly as in previous studies[116, 117]. The task design was made up of five activation blocks and five baseline blocks each lasting 45 seconds, alternating. The blocks were introduced by relevant single words using the headphone designed especially for fMRI (NordicNeuroLab,

Bergen, Norway). The proper sound volume was adjusted before the examination. The task was explained to the participants in detail before scanning and an individual hometown walk encompassing a central point, main landmarks as destinations was prepared. During the active block the subjects were asked to mentally navigate through the different routes among landmarks and to imagine as many details as possible while navigating. Subjects were instructed to look around if they reached the destination before the baseline condition. After 45 seconds, each route was interrupted by the baseline task. The baseline condition consisted of covertly counting odd numbers starting with 21 to hold patients back from further spontaneous mental navigation and to avoid the possible disturbing effect of the attention caused contrast.

Covert word generation task paradigm

This task involved alternating active covert word generation and passive resting state periods in a block design as presented earlier[118, 119]. Both periods lasted 30 seconds and the cycles were repeated seven times. The beginning of an active period was cued by a certain letter that was given to the subject via a headphone designed for fMRI. During active condition, subjects were asked to mutedly generate as many words as possible beginning with the given letter. The end of the active period was indicated as well. The patients were asked not to move at all, including pronunciation during the examination and were observed through a camera for further confirmation. To avoid disturbing effects of visual processing and linked functions such as working memory, the patients were told to keep eyes closed.

Data processing

Diffusion tensor imaging and Tract-Based Spatial Statistics (TBSS)

Initial diffusion image processing was carried out to generate Tract-Based Spatial Statistics (TBSS) input data using the FDT tool (FMRIB's Diffusion Toolbox), part of FSL (FMRIB's Software Library, www.fmrib.ox.ac.uk/fsl)[120]. The steps included eddy current correction and motion correction using a 12 parameter affine registration to a reference volume (i.e. non diffusion weighted data, b = 0 s/mm2), averaging of the four sets of 20 diffusion directions and automated brain extraction with BET (Brain Extraction Tool)[121], which was manually supervised to avoid incorrect brain extraction. Diffusion data was then fed into DTIFit[120] to calculate the diffusion tensor model for each brain voxel and subsequently to compute FA and MD values from the tensor's three eigenvalues[122].

Voxelwise statistical analysis of the FA data was carried out using TBSS[123], part of FSL[120]. TBSS projects all subjects' FA data onto a mean FA tract skeleton in standard space, before applying voxelwise cross-timepoint or cross-group statistics. We run TBSS for other diffusion-derived data, MD as well. The voxelwise statistics were performed on skeletonized data using the permutation-based non-parametric Randomize analysis, involved in FSL[124]. The two time point FA and MD data from both mTBI and control groups were compared by non-parametric paired t-test to maximize statistical power. We compared the mTBI to control group by non-parametric unpaired t-test, in both first and second time points. Results were considered significant for $p < 0.05$, corrected for multiple comparisons using „threshold-free cluster enhancement", which avoids making an

arbitrary choice of the cluster-forming threshold, while preserving the sensitivity benefits of clusterwise correction.

Volumetric analysis

T1-weighted high resolution images were fed into volumetric segmentation that was performed with the FreeSurfer image analysis suite (Athinoula A. Martinos Center for Biomedical Imaging, 2005)[125-131]. This processing includes the removal of non-brain tissue using a hybrid watershed/surface deformation procedure[131], automated Talairach transformation, segmentation of the subcortical white matter and deep gray matter volumetric structures[127, 132], intensity normalization[133], tessellation of the gray matter-white matter boundary, automated topology correction[134, 135], and surface deformation following intensity gradients to optimally place the gray/white and gray/CSF borders at the location where the greatest shift in intensity defines the transition to the other tissue class[125, 126, 136]. Each of the following steps were checked: the Talairach transform, the accuracy of the skull strip, the accuracy of the white matter and pial surface segmentation. Corrections were performed when necessary. The output volumes of cortex, white matter, corpus callosum, ventricles, extracerebral CSF, hippocampus, amygdala, pallidum, caudate nucleus, thalamus, and nucleus accumbens were statistically compared between first and second time point by simple paired t-test, both in traumatic and control groups. Analysis between patient and control groups was carried out using unpaired t-test on volumes normalized to ICV.

Longitudinal brain volume change calculation and illustration were carried out on MPRAGE images using FSL "SIENA" package [120] . First, percentage brain volume changes between two time points were estimated. Next, for each subject, the edge displacement image (encoding, at brain/non-brain edge points, the outwards or inwards edge change between the two time points) was dilated, transformed into MNI152 (Montreal Neurological Institute and Hospital developed standard space, http://nist.mni.mcgill.ca/?page_id=714) space, and masked by a standard MNI152-space brain edge image. This way the edge displacement values were warped onto the standard brain edge[137]. Next, the resulting images from all subjects were fed into voxelwise statistical analysis using Randomize tool[124] (non-parametric paired t-test, results were considered significant for $p < 0.05$, corrected for multiple comparisons using „threshold-free cluster enhancement") to test brain volume change in the traumatic and control group between the 72h and one month measurements.

Susceptibility weighted imaging

Susceptibility weighted images were searched for hemorrhagic lesions by a board-certified neuroradiologist.

Functional MRI

Pre-processing and statistical analysis were performed using FEAT (FMRI Expert Analysis Tool) Version 5.98, part of FSL. Pre-processing included BET (brain extraction tool, part of FSL)[138],

MCFLIRT (motion correction FMRIB's linear image registration tool)[139], spatial smoothing with 5 mm full width at half maximum and high-pass temporal filtering with 120 s cut-off. The temporal filtering applied to the data was used for the model as well. Whole brain general linear model (GLM) time-series statistical analyses of individual data sets were carried out using FILM (FMRIB's Improved Linear Model) with local autocorrelation correction[140]. To model the BOLD response a box-car function with "task" vs. "rest" conditions was convolved with the FSL's canonical gamma haemodynamic response function (HRF). The temporal derivative of this waveform was also included in our design-matrix to correct for slight overall temporal shifts between the model and the data.

Single session data sets were registered into standard space using a three-step process. First, low-resolution fMRI data from each subject were registered to that subject's (brain-extracted) high-resolution T1 weighted structural image (7 degrees-of-freedom linear fit). Second, the high-resolution image was registered to the MNI152 standard brain image (12 degrees-of-freedom linear fit) using FLIRT (FMRIB's linear image registration tool)[139]. Third, the registration from structural image to the standard space was further refined using FNIRT (FMRIB's non-linear image registration tool)[141, 142]. The resulting linear and non-linear deformations were combined mathematically and applied to the first-level statistical maps to take them into standard space. Interpolation was only used for the final step, not in the registration calculations.

Next, second-level mixed effects analysis was carried out using the first level statistical maps to test for mean group activations within group changes over the one-month period and differences between the control and mTBI groups. For a more accurate group analysis, the option FLAME (FMRIB's Local Analysis of Mixed Effects) with both stages (FLAME 1+2) was chosen. This option

includes a full MCMC (Markov Chain Monte Carlo sampling) based analysis of voxels close to threshold that is advantageous at small sample sizes (n < 10). To calculate group average activation maps (e.g. < 72h acquisition in mTBI group) the “single group average” model was set up. Group average deactivation maps were also produced. When calculating extraction based contrast maps between time points of one group (e.g. < 72h data minus 1 month data and vice versa in mTBI group) the “two groups, paired” design was applied (paired t-test). When calculating contrast maps between groups (control group minus mTBI group and vice versa at both < 72h and 1 month) the “two groups, unpaired” design was selected (unpaired t-test). Average activation maps for both groups at both time points and contrast maps of all possible variations were calculated.

Statistical map thresholds were set using clusters determined by $Z > 2.3$ and a corrected cluster significance of $p < 0.05$[143].

3.2 Results

Structural images

T1- and T2-weighted structural images were found to be free of trauma related pathology.

No low-signal foci referring to microhemorrhages were apparent on the SWI in the traumatic or in the control group.

Tract-Based Spatial Statistics

Longitudinal analysis:

TBSS analysis between 72h and one month acquisition of traumatic patients showed significant difference (corrected $p < 0.05$) in voxels of anterior corpus callosum, right corona radiata and internal capsule for both FA and MD values. FA was lower, while MD was higher at 72 h than after one month (see **Fig. 3.2.1.** and **Table 3.2.1.** for details). No voxels appeared to be significant on the opposite contrasts (72h > 1 month for FA, one month > 72h for MD). The two time point comparison of control subjects revealed no statistical difference regarding MD or FA.

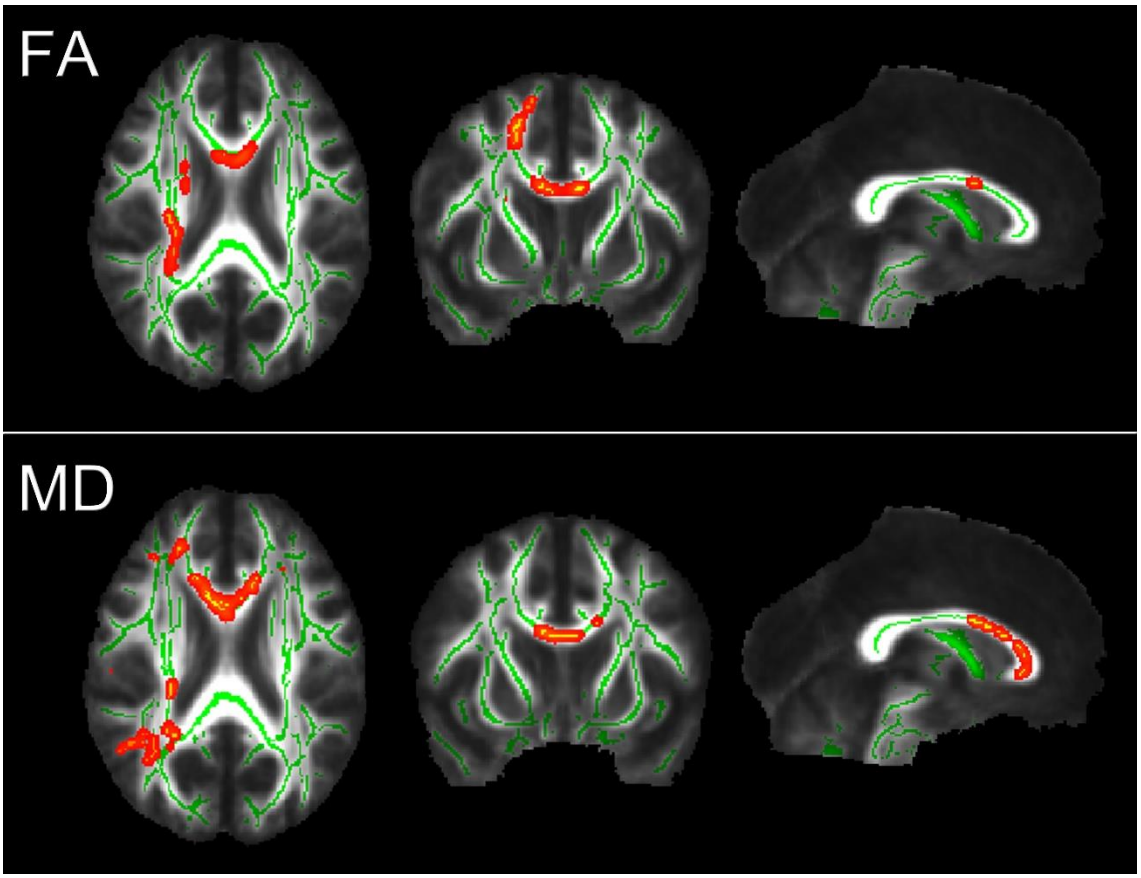

Fig. 3.2.1. Results of the Tract-Based Spatial Statistics (TBSS) analysis of the 72h and 1 month data of the mTBI group. The red-yellow voxels represent significantly (corrected $p < 0.05$) decreased fractional anisotropy (FA) and increased mean diffusivity (MD) values in the 72h data compared to the one month data. Significant voxels are thickened into local tracts and overlaid on the group mean WM skeleton (green), and the group mean fractional anisotropy (FA) image (grayscale). Images are shown in radiological convention (right = subject's left). Slice coordinates (MNI 152 aligned anatomical): x = 0 mm, y = 10 mm, z = 22 mm

Cross-sectional analysis: imaging within 72h after injury:

Comparison between the mTBI group's 72h imaging and the control group's first time point imaging showed FA to be significantly decreased (corrected $p < 0.05$) and MD to be significantly increased (corrected $p < 0.05$) in the traumatic group diffusely in several white matter tracts of both hemispheres (see **Fig. 3.2.2.** and **Table 3.2.1.** for details). The contrast of control group MD minus mTBI group MD, or mTBI group FA minus control group FA yielded no significant voxels.

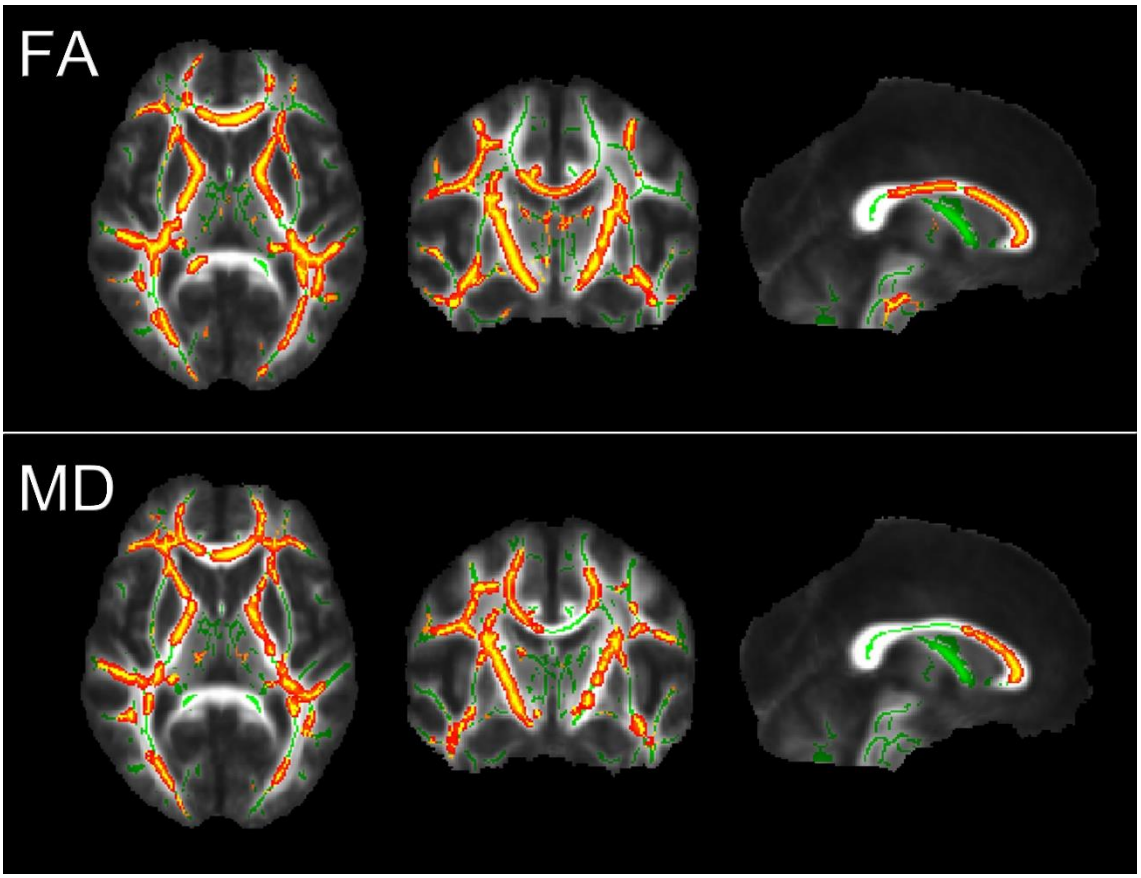

Fig. 3.2.2. Results of the Tract-Based Spatial Statistics (TBSS) analysis of the control and mTBI group at the 72h. The red-yellow voxels represent significantly (corrected $p < 0.05$) decreased fractional anisotropy (FA) and increased mean diffusivity (MD) in the mTBI group compared to the control group. Significant voxels are thickened into local tracts and overlaid on the group mean WM skeleton (green), and the group mean fractional anisotropy (FA) image (grayscale). Images are shown in radiological convention (right =subject's left). Slice coordinates (MNI 152 aligned anatomical): x = 0 mm, y = -10 mm, z = 7 mm

Cross-sectional analysis: imaging at one month:

The comparison of mTBI group data at one month to control group data at the second time point also highlighted significantly (corrected $p < 0.05$) reduced FA in the mTBI group, but only in the right hemispherium, in much smaller extent (see **Fig. 3.2.3.** and **Table 3.2.1.** for details). The opposite contrast did not reveal any significant results. MD values showed changes in the opposite direction as FA values, but without reaching statistical significance.

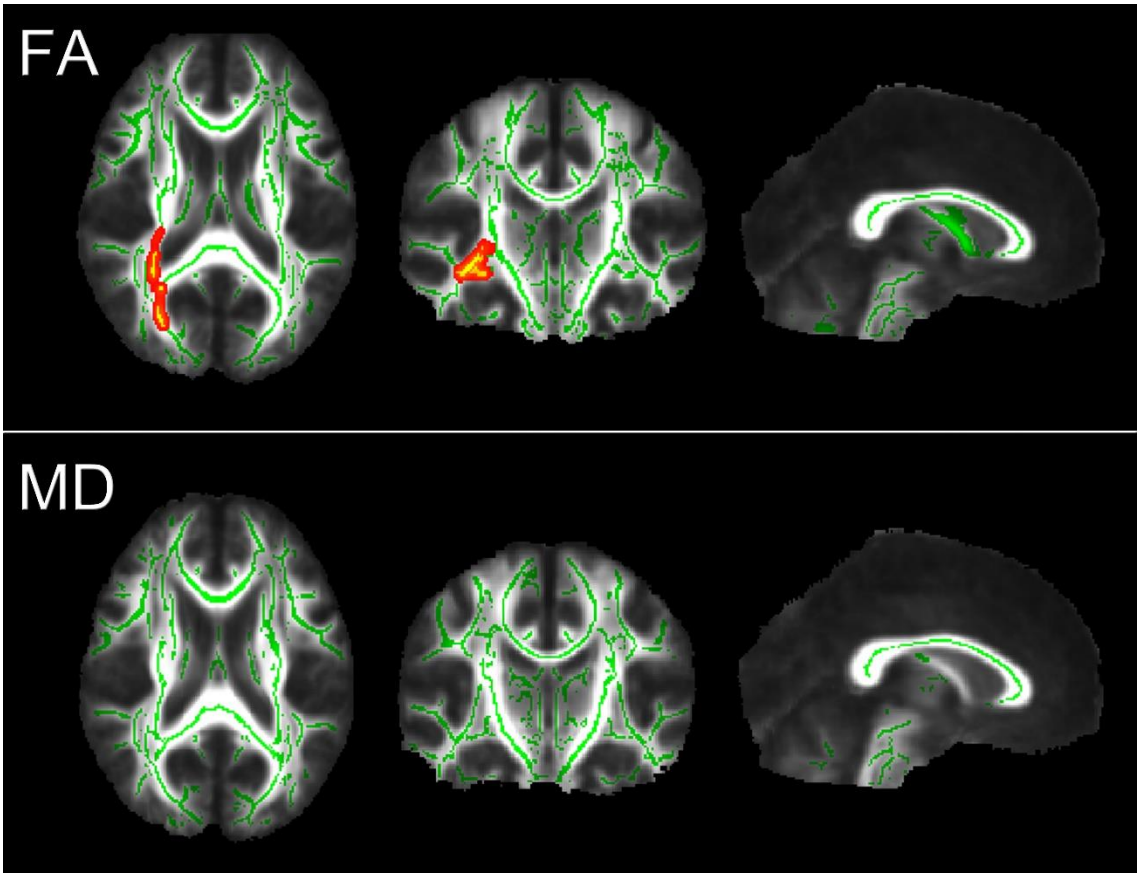

Fig. 3.2.3. Results of the Tract-Based Spatial Statistics (TBSS) analysis of the control group and mTBI group at one month. The red-yellow voxels represent significantly (corrected $p < 0.05$) decreased fractional anisotropy (FA) in the mTBI group compared to the control group. Significant voxels are thickened into local tracts and overlaid on the group mean WM skeleton (green), and the group mean fractional anisotropy (FA) image (grayscale). Images are shown in radiological convention (righ = subject's left). Slice coordinates (MNI 152 aligned anatomical): x = 0 mm, y = -17 mm, z = 19 mm

Table 3.2.1.

Details of significant (corrected p < 0.05) voxels yielded by TBSS

Contrast	Voxel no.	Average [a]		p [b]
		72h	1 month	
		FA		
mTBI 72h < mTBI 1 month	3408	0.5653	0.5883	0,041
		mTBI	Control	
mTBI 72h < Control	40737	0.4994	0.548	0,01
mTBI 1 month < Control	1932	0.5541	0.612	0,045
		MD[c]		
mTBI 72h > mTBI 1 month	7450	8.12	7.7	0,032
		mTBI	Control	
mTBI 72h > Control	39078	7.9	7.36	0,005
mTBI 1 month > Control	0	-	-	0,084

[a]Average values of subjects' white matter "skeleton" voxels that were yielded significantly different in given contrast. [b]P value for voxel with highest statistical difference [c]10^{-4} mm^2/sec.

Fig. 3.2.4 illustrates the relations of FA and MD values found across sessions and groups.

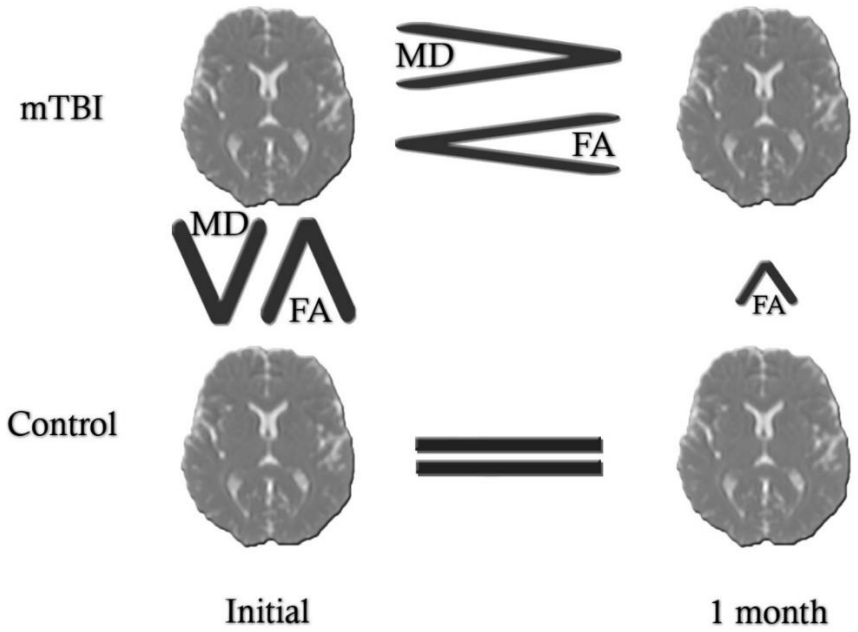

Fig. 3.2.4. Illustration of relations of FA and MD values

Volumetric analysis

FreeSurfer volumetric segmentation:

Significant differences ($p < 0.05$) were detected between the 72h and one month volumes of the cortex, ventricles and extracerebral CSF in the mTBI group. Cortical grey matter volume at 72h was larger than at one month. Ventricular (more pronouncedly lateral ventricle) and extracerebral CSF volume was lower at 72h. No significant volume change over time was found in other investigated structures such as white matter, hippocampus, amygdala, pallidum, caudate nucleus, nucleus accumbens and thalamus. The average loss of cortical volume over one month was 1.02%. Gain of average ventricular volume over time was 3.4%. Volume changes in control group were not significant. **Table 3.2.2.** shows details of longitudinal brain structure volume comparison in the mTBI and control groups. Cross-sectional comparison of any normalized (to ICV) brain structure volumes revealed no significant difference between control and traumatic group either at 72h or one month, see **Table 3.2.3**.

Table 3.2.2.

Longitudinal comparison of brain structure volumes (µl) in mTBI and control groups

	mTBI			Control		
Structure	72h Mean (SD)	1 month Mean (SD)	p[a]	Initial Mean (SD)	1 month Mean (SD)	p[a]
Cortical GM	**474917 (69264)**	**470068 (65550)**	**0,029**	479175 (52835)	478777 (51015)	0,44
Ventricles	**20198 (16545)**	**20882 (16830)**	**0,023**	20860 (16443)	20920 (16151)	0,38
Lateral ventricles	**16857 (14736)**	**17558 (15075)**	**0,007**	17160 (14800)	17212 (14717)	0,34
E.C. CSF	**1402 (572)**	**1466 (597)**	**0,013**	1436 (315)	1444 (300)	0,3

E.C. CSF = Extra cerebral cerebrospinal fluid; GM = Grey matter; SD = Standard deviation [a]Paired t-test

Table 3.2.3.

Comparison of brain structure volumes between mTBI and control subjects

	mTBI 72h		mTBI 1 month		Control
Structure	Mean (SD)	p[a]	Mean (SD)	p[a]	Mean (SD)
Cortical GM /ICV	0,3601(0,0424)	0,41	0,3569 (0,0409)	0,49	0,3568 (0,0352)
Ventricles/ICV	0,0148 (0,0111)	0,47	0,0153 (0,0114)	0,43	0,0145 (0,0104)
Lateral ventricles/ICV	0,0123 (0,0099)	0,45	0,0129 (0,0102)	0,40	0,01189 (0,0097)
E.C. CSF/ICV	0,00105 (0,00039)	0,47	0,00110 (0,00041)	0,32	0,00104 (0,00019)

E.C. CSF = Extra cerebral cerebrospinal fluid; GM = Grey matter; ICV = Intracranial volume; SD = Standard deviation [a]Unpaired t-test

FSL SIENA:

Analysis of edge displacement data (edge flow) showed significant outwards edge movement in several voxels lining the 3rd and the lateral ventricles from the 72h to one month imaging in the traumatic group, as it is presented on **Fig. 3.2.5.** Opposite edge displacement (inwards) or edge displacements in control group were not significant.

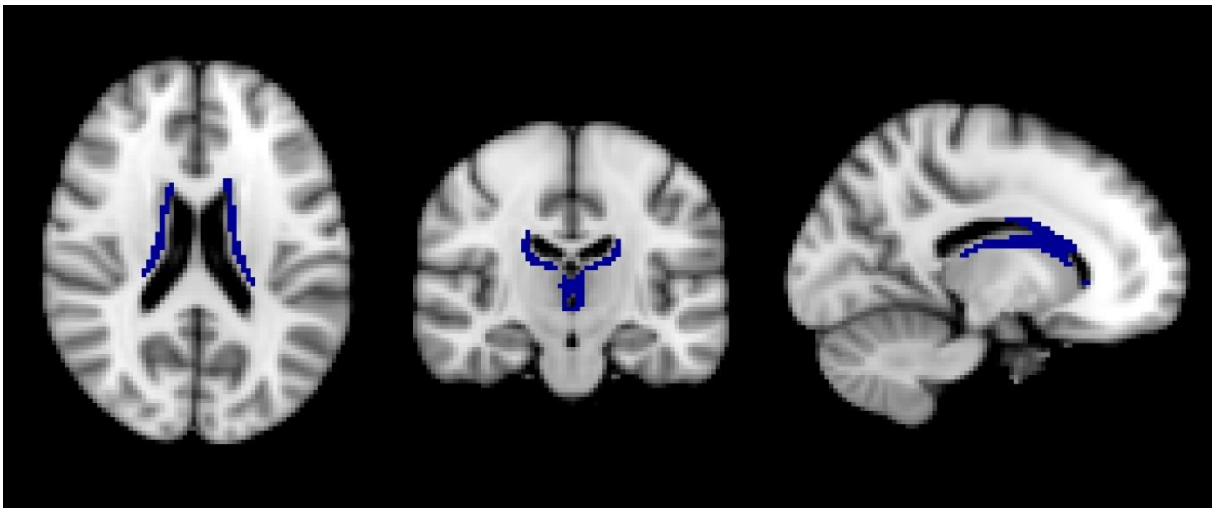

Fig. 3.2.5. Results of voxel based multi-subject SIENA analyis in the mTBI group. Blue voxels indicate significant ($p < 0.05$) outward edge displacement over time in the traumatic group. Slice coordinates in MNI 152 space: x = -14 y = -18 z = 20

Functional MRI

All participants were able to perform the fMRI tasks and gave feedback reporting that they had performed the tasks according to the instructions given.

Cortical patterns during hometown walking task:

Average activation map of the mTBI group at <72h is presented on **Fig. 3.2.6.** Activation was detected bilaterally in the parahippocampal gyri, temporal fusiform cortex, precuneus cortex and lateral occipital cortex; details are listed in T**able 3.2.4**. No marked difference appeared by visual inspection when comparing the <72h average activation map to the activation map at 1 month, or to activation map of the control group at any time point.

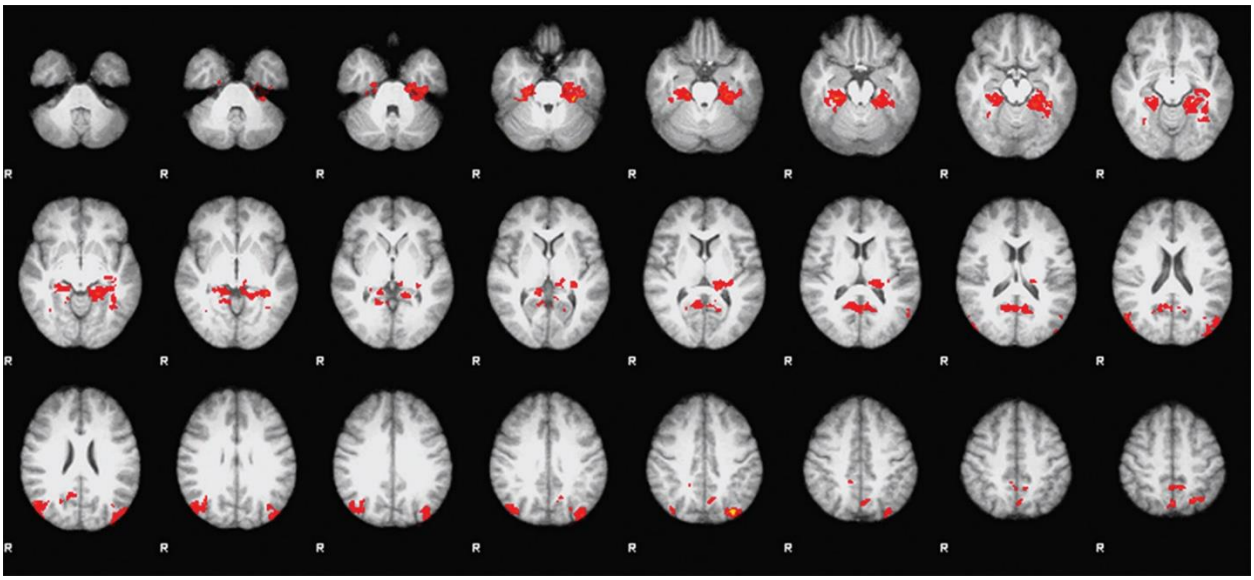

Figure. 3.2.6. Average activation map related to hometown walking task of the mTBI group at <72h after injury. Significant clusters (red-yellow, $Z > 2.3$, $p < 0.05$) are overlaid on standard MNI 152 brain images. Cortical activation clusters appear in bilateral parahippocampal gyri, temporal fusiform cortex, precuneus cortex and lateral occipital cortex. Images follow radiological convention (R = Subjects right).

Longitudinal analysis, i.e. contrast of <72h and 1 month images of the traumatic group revealed significantly ($Z > 2.3$, $p < 0.05$) higher BOLD signal at 1 month bilaterally in voxels of the parahippocampal gyri and temporal pole (**Fig. 3.2.7.**). Details are listed in **table 3.2.4**. BOLD signal was not significantly higher in any voxels at the <72h acquisition.

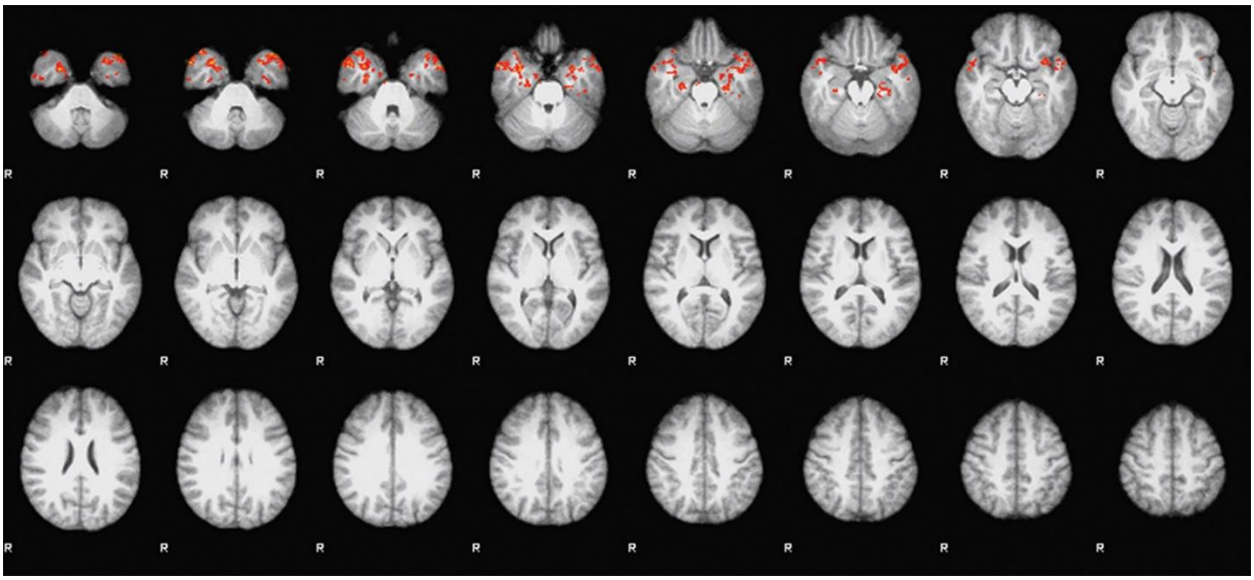

Figure. 3.2.7. Comparison of <72h and 1 month activation related to hometown walking task in the mTBI group. Red-yellow clusters (overlaid on MNI 152 standard brain) represent brain regions where significantly ($Z > 2.3$, $p < 0.05$) higher BOLD signal was observed at 1 month compared to <72h. These clusters are located bilaterally in the parahippocampal gyri and the temporal pole. Images follow radiological convention (R = Subjects right).

In the control group, apart from a subtle cluster (275 voxels) referring to significantly ($Z > 2.3$, $p < 0.05$) higher BOLD signal at the first acquisition compared to the second at the occipital lobe (**table 3.2.4**.), no significant differences were observed between the first and second measures. The contrast of mTBI and control data revealed no significant ($Z > 2.3$, $p < 0.05$) differences in BOLD signal.

Table 3.2.4.

Local maxima related to hometown walking task

Analysis	Cluster	Voxel#	Z max	x	y	z	Anatomical area
mTBI 72h	1	2212	9.29	-20	-40	-18	Parahippocampal gyrus p.d. (L)
			7.02	-28	-32	-26	Temporal fusiform cortex p.d. (L)
			5.64	-22	-16	-30	Parahippocampal gyrus a.d. (L)
	2	1591	6.54	20	-34	-18	Parahippocampal gyrus p.d. (R)
			5.37	30	-32	-20	Temporal fusiform cortex p.d. (R)
			4.6	22	-16	-30	Parahippocampal gyrus a.d. (R)
	3	648	6.06	0	-68	54	Precuneus cortex
	4	505	5.78	-34	-76	42	Lateral occipital cortex s.d. (L)
	5	451	4.37	50	-70	36	Lateral occipital cortex s.d. (R)
mTBI 72h > 1 month	-	-	-	-	-	-	-
mTBI 1 month > 72h	1	1415	4.22	54	10	-36	Temporal pole (R)
			2.9	16	-6	-28	Parahippocampal gyrus a.d. (R)
	2	1333	3.82	-54	6	-32	Temporal pole (L)
			3.36	-20	-18	-28	Parahippocampal gyrus a.d. (L)
			2.65	-18	-32	-20	Parahippocampal gyrus p.d. (L)
Control 1st > 2nd	1	275	3.6	16	-88	46	Occipital pole
Control 2nd > 1st	-	-	-	-	-	-	-

List of local maxima in group analyses related to hometown walking task cortical activations. The x-, *y*- and *z*-values correspond to the MNI coordinates of local maxima in mm. More local maxima are reported in each cluster when the cluster encompasses more than one anatomical location. L = left hemisphere, R = right hemisphere, a.d. = anterior division, p.d. = posterior division, s.d. = superior division.

Cortical patterns during covert word generation task:

Covert word generation task related average activation map of the mTBI group at <72h is presented on **Fig. 3.2.8.** Activation was detected in the left inferior frontal gyrus triangular and opercular part (Broca area), frontal orbital cortex, supplementary motor area, right insula and cingulate gyrus, see **table 3.2.5**. Subcortical activations occurred in the caudate nucleus, thalamic nuclei, putamen and pallidum bilaterally. No marked difference appeared by visual inspection when comparing the <72h average activation map to the activation map at 1 month, or to activation map of the control group at any time point.

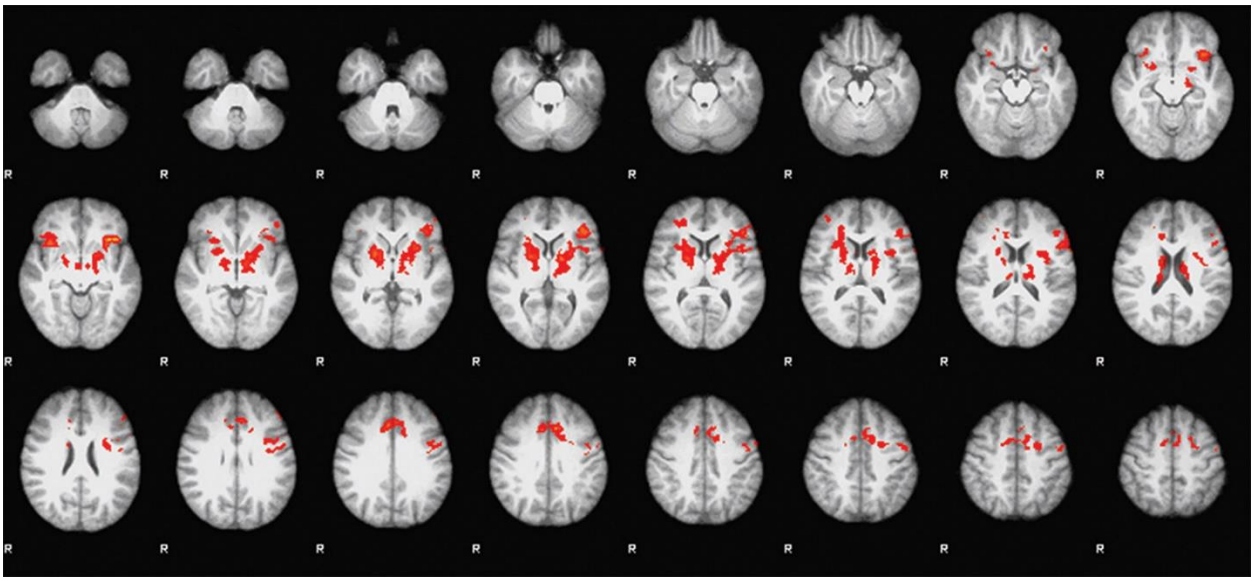

Figure. 3.2.8. Average activation map related to covert word generation task of the mTBI group at <72h after injury. Significant clusters (red-yellow, $Z > 2.3$, $p < 0.05$) are overlaid on standard MNI 152 brain images. Cortical activation clusters appear the left inferior frontal gyrus triangular and opercular part (Broca area), frontal orbital cortex, supplementary motor area, right insula and cingulate gyrus. Images follow radiological convention (R = Subjects right).

Contrast of the <72h and 1 month measurements of the traumatic group revealed significantly ($Z > 2.3$, $p < 0.05$) higher BOLD signal at <72h compared to 1 month mainly in the medial prefrontal cortex (**Fig. 3.2.9.**). Exact locations are presented in **table 3.2.5**. The opposite contrast, i.e. 1 month data minus <72h data showed no significant results.

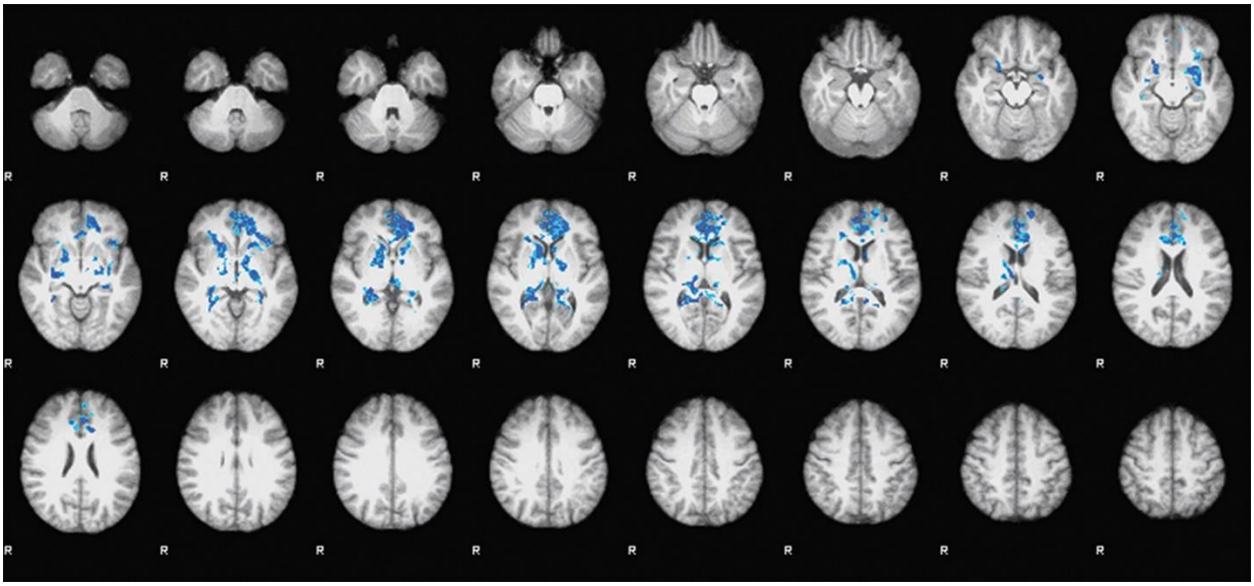

Figure 3.2.9. Comparison of <72h and 1 month activation related to covert word generation task in the mTBI group. Blue-light blue clusters (overlaid on MNI 152 standard brain) represent brain regions where significantly ($Z > 2.3$, $p < 0.05$) higher BOLD signal was observed at <72h compared to 1 month. These clusters are located in the medial prefrontal cortex and cingulate gyrus posterior division. Images follow radiological convention (R = Subjects right).

The contrasts of the two time point data in the control group can be seen on **Fig. 3.2.10**. First time point minus second showed significant ($Z > 2.3$, $p < 0.05$) difference in BOLD signal in the right frontal opercular cortex and left subcortical areas. Second time point minus first showed

significant difference in the left anterior hippocampus. Cluster details are included in **Table 3.2.5**. The contrast of mTBI and control data has revealed no significant ($Z > 2.3$, $p < 0.05$) differences.

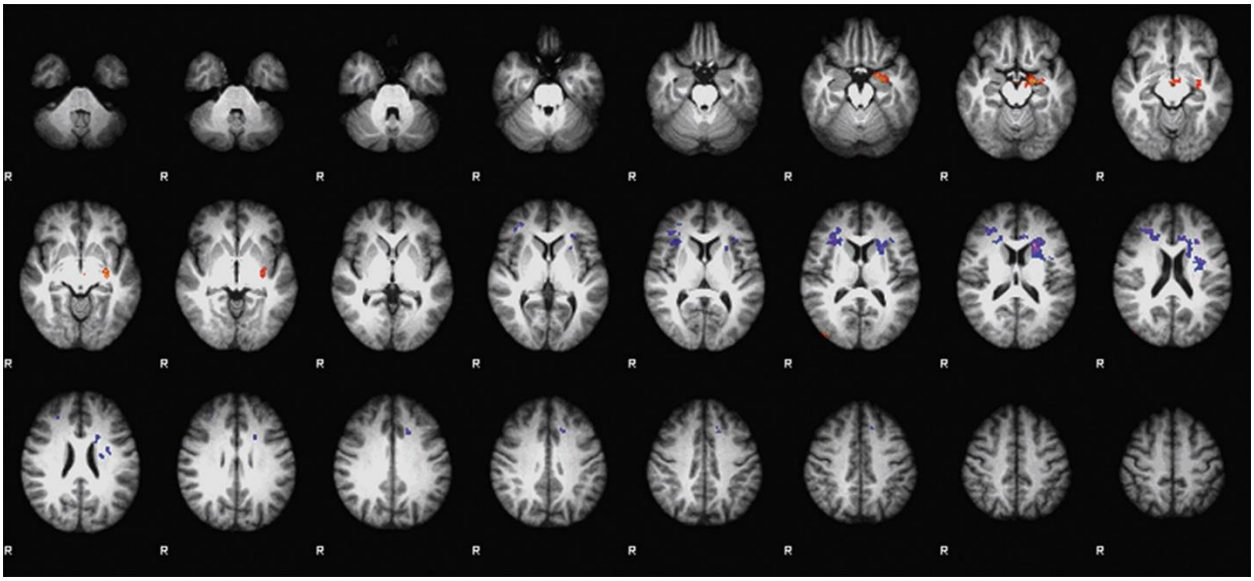

Figure 3.2.10. Comparison of first and second time point activation related to covert word generation task in the control group. Red-yellow clusters (overlaid on MNI 152 standard brain) represent brain regions where significantly ($Z > 2.3$, $p < 0.05$) higher BOLD signal was observed at the second time point compared to the first. These clusters are located in the left anterior hippocampus. Blue-light blue clusters represent brain regions where significantly ($Z > 2.3$, $p < 0.05$) higher BOLD signal was observed at the first time point compared to the second. These clusters are located in the right frontal opercular cortex. Images follow radiological convention (R = Subjects right).

Table 3.2.5.

Local maxima related to covert word generation task

Analysis	Cluster	Voxel#	Z max	x	y	z	Anatomical area
mTBI 72h	1	3067	8.31	-52	-2	46	Precentral gyrus (L)
			8.1	-32	22	-10	Frontal orbital cortex (L)
			8.0	-40	34	4	Inf. Frontal gyrus triangular part (L)
			3.6	-54	16	14	Inf. Frontal gyrus opercular part (L)
	2	2901	9.14	-2	-4	60	Supplementary motor area (L)
			8.18	38	18	-8	Insula (R)
			7.63	8	18	34	Cingulate gyrus a.d. (R)
mTBI 72h > 1 month	1	1485	4.89	-16	58	14	Frontal pole (L)
			4.68	-10	50	-4	Medial prefrontal cortex (L)
	2	512	5.01	22	-46	6	Cingulate gyrus p.d. (R)
MTBI 1 month > 72h	-	-	-	-	-	-	-
Control 1st > 2nd	1	353	3.78	36	22	10	Frontal opercular cortex (R)
Control 2nd > 1st	1	318	3.98	-20	-10	-16	Hippocampus (L)
			3.2	-22	0	-28	Parahippocampal gyrus a.d. (L)

List of local maxima in group analyses related to covert word generation task cortical activations. The *x*-, *y*- and *z*-values correspond to the MNI coordinates of local maxima in mm. More local maxima are reported in each cluster when the cluster encompasses more than one anatomical location. L = left hemisphere, R = right hemispheres, a.d. = anterior division, p.d. = posterior division, inf. = inferior

The deactivation average maps at <72h and 1 month are presented in **fig. 3.2.11**. A smaller extent of deactivation at <72h compared to 1 month is evident.

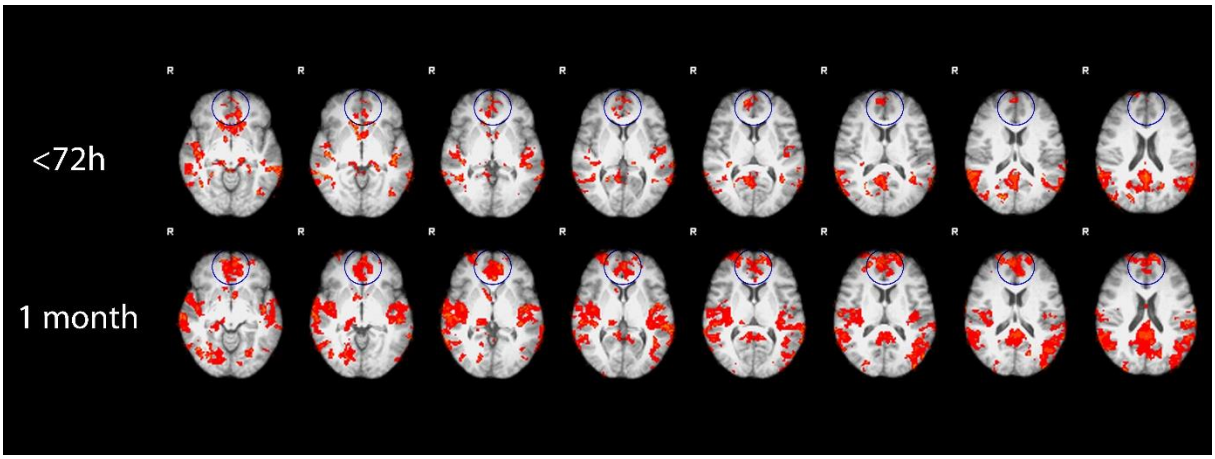

Figure 3.2.11. Deactivation average maps of the mTBI group during covert word generation at <72h and 1 month after injury, focusing on the medial prefrontal cortex (blue circle). A deactivation of smaller extent can be seen at <72h (first row). Images follow radiological convention (R = Subjects right).

3.3 Discussion

These studies investigated the structural alterations detectable by DTI, volumetric analysis and SWI, and also functional changes detectable by fMRI in a longitudinal set after mTBI. We found marked differences in microstructure and brain volumes between the acute and sub-acute state by DTI and volumetric analysis, and characteristic functional activation and deactivation

alterations. We suppose that these changes over time provide an insight to structural-functional alterations and regeneration following mTBI.

Diffusion tensor imaging

We found DTI parameters FA and MD to substantially differ between the acute phase mTBI patients and control subjects in nearly all white matter tracts. Mild TBI patients showed decreased FA values, and oppositely, increased MD values (which is not surprising considering the theoretically opposite denotation of these indices) compared to healthy subjects. After one month, this difference to controls remained only to a distinctly smaller extent –limited to nearly 20 times less voxels in the right hemisphere regarding FA, and got insignificant regarding MD. The approach of DTI values to normal was also presented by the longitudinal analysis, which yielded significant increase of FA, and significant decrease of MD in the mTBI group over one month. The DTI parameters remained reliably constant in the control group across the two acquisitions.

Overall, these findings suggest that the DTI-detectable abnormality developing in the acute phase is resolving dynamically in the first month after mild injury.

The exact mechanisms behind the detected changes of DTI indices remain still elusive. Due to different observations, DTI parameters of the brain following TBI are related to a complex set-up of dependent and independent factors. Axonal and myelin sheath pathology, ratio of extracellular and intracellular water compartments linked to edema or cell death together have an effect on the diffusion tensor. Many studies reporting reduced FA or elevated MD of mild

traumatic patients explain this type of alteration with reduced integrity i.e. misalignment of axonal and myelin structures as a consequence of shear-strain forces, including local expansion of the axonal cylinder, or axonal disconnection[55, 61, 144]. On the other hand, some more recent studies observed elevated FA or reduced MD short after mild injury along several white matter regions[56, 145, 146]. One possible underlying mechanism is cytotoxic edema, as in this condition the injury induced altered function of gated ion channels results in intracellular swelling and decrease in extracellular water that causes reduced radial diffusivity[53, 147, 148]. The output yielded by DTI may be a summarized effect of the two basic mechanisms, microstructural disintegration and cytotoxic edema.

The actual dominance of these substantial mechanisms in the white matter may theoretically depend on temporal, spatial factors, attributes of the patient and the circumstances of injury[149]. Although a recent study presenting bidirectional changes in FA of mTBI patients raised the possibility of spatial factors contributing to alterations in FA[150], our data rather support the significance of temporal factors. Both FA and MD changed significantly in a relatively short period, and no bidirectional changes were detected. The rapid consolidation of MD hypothetically may be associated with the recovery process from edema, since edema is thought to pass over in a similar pace after mTBI[151, 152]. However, the insignificant difference in MD values driven by TBSS between one month mTBI patients and controls do not necessarily mean normal MD values for the patients at one month. Furthermore, FA remained significantly reduced in different white matter regions after one month. This is somewhat surprising regarding that FA is thought to be more variable among subjects and thus potentially less sensitive[153]. However, this type of slower

consolidation of FA values may mirror a process of cellular re-alignment and a clean-up of degenerative residuals by phagocytes.

Considering that FA and MD are averaged parameters resulting from the eigenvectors and eigenvalues, some important characteristics of microstructure may get hidden. A separate investigation of the eigenvectors and eigenvalues in mTBI may help to better understand the correlation between DTI indices and underlying pathology.

Beyond the theoretical considerations, the most important practical implication of our findings is that the timing of DTI acquisition plays a crucial role in the results, and needs to be considered when interpreting the data. We suggest a standardized DTI timing is needed for future clinical application.

Volumetric analysis

The volumetric analyses demonstrated significant reduction of gray matter volume accompanied by significant CSF volume gain over one month after mTBI. Overall, these changes indicate reduction of brain tissue volume, which may be a consequence of both the recovery from initial subtle edema and the initiation of atrophy. To elucidate the contribution of these two factors, cross-sectional analysis was carried out, which, surprisingly yielded no significant differences between the control and the TBI group at any time points.

This is probably the kickback of the high inter-subject variability of brain structure volumes, and that of the low number of subjects, also observed as an obstacle in a previous volumetric study[85]. Previously, Warner et al.[154] found lateral ventricle volumes to be significantly smaller in acute TBI

patients than in control subjects. This supports the theory that acute edema formation (brain swelling) may take place in TBI patients. Nevertheless, the presence of volumetric changes detectable over the first month mandates further investigations.

Both the amount of brain swelling and the subsequent atrophy correlates with clinical severity and outcome as described in previous studies[85, 152, 155-157]. Hence, the rate of brain volume change at the acute – to sub-acute stage is likely to have prognostic value as it represents the effect of impact and the following degeneration. Furthermore, based on the inter-session sensitivity of Freesurfer volumetric segmentation presented here, MRI volumetric analysis may be applied as a non-invasive tool in measuring brain edema retrospectively at an optimal interval after injury. Our data showed lateral ventricles to be the structures with the most potential for detecting volume changes after injury.

Susceptibility weighted imaging

Although compared to other imaging methods, SWI is extremely sensitive to microhemorrhages and reveals a high number of them in severe to moderate TBI[73], microhemorrhages do not seem to be frequent in mTBI[74]. Thus the absence of detectable microhemorrhages is not surprising in the very mildly injured group presented here. SWI may be implemented to sub-classify mTBI, declaring microhemorrhage positive or negative cases. This distinction may be helpful when interpreting DTI results in mTBI, as in this study, SWI data ensured that DTI data were not influenced by hemorrhagic lesions.

Functional MRI

Hometown walking task

Hometown walking task is aimed to assess visuo-spatial memory retrieval process and this type of function is known to be one of the most efficient in activating bilateral mesiotemporal structures, particularly the parahippocampal gyrus[158-161]. This task was proved to be robust enough and is also performable by children or patients with a slight cognitive impairment[116, 161], representing a potential tool in the assessment of mesiotemporal structures in mTBI at an early phase.

The cortical patterns of either individual images or group averages were similar to the expected patterns[116, 161]. Qualitative differences between activation patterns of traumatic and control subjects were not apparent by visual inspection. Instead, longitudinal analysis performed on the mTBI group revealed significantly lower activation at the acute time point (<72h) compared to the one month delayed time point. This hypoactivation was located in structures that are involved during the hometown walking task, most importantly in the parahippocampal gyrus. Unlike in the mTBI group, the comparison of the two time points of the control group showed no relevant difference, proving the reproducibility of this task and excluding that any additional activation pattern is generated by the repetition itself.

Somewhat surprisingly no significant difference was seen on the cross-sectional analyses, either at <72h or 1 month. A possible cause of this is the relatively high inter-subject variance of cortical patterns in fMRI examinations as demonstrated earlier[162]. Because of the lack of cross sectional data, the cortical pattern alteration detected in the traumatic group over time remains relative.

However, we supposed that the <72h hypoactivation represents the pathological state followed by a partial or total recovery as similar outcome was reported by others[103]. The finding of reduced activation following injury is congruent with a branch of previous studies, although these investigators focused on working memory tasks and the reduced activation patterns were found in the dorsolateral prefrontal cortex, a locus known to be responsible for working memory functions[92, 103, 163]. One study concentrating on the medial temporal lobe by cognitive tests and n-back task presented inverse correlation of symptom severity in mTBI and activation level in the MTL, particularly the hippocampus[98]. This study also joined the theory that MTL injury underlies memory dysfunctions. Although it is not possible to record task performance during hometown walking, the hypoactivation located at the parahippocampus and temporal areas itself may be regarded as an additional possible cause of memory disturbance following mTBI.

The underlying mechanism is likely to be associated with axonal damage, namely DAI that was demonstrated by a wide range of studies using DTI[150]. Axonal disruption and- swelling may lead to impaired axonal potentials, and so purportedly also explain the abnormal activation patterns related to hometown walking task in our study.

Covert word generation task

The covert word generation task, also applied in our study, similarly to the hometown walking task, is a robust and easily conductible task that can also be performed on brain injured patients with cognitive deficit[164]. This paradigm was originally developed to localize language production and lateralization, and is often used to exchange Wada test[118, 165].

In the present study, we used this task to investigate the effect of mTBI on cortical patterns during such essential function as language production. The fMRI results of individual and group averages both in traumatic and control subjects validated that the task was performed properly since typical areas of activations appeared[166]. Similarly as in hometown walking task, no marked difference was apparent on functional images of traumatic and control subjects, instead, group analyses were required to reveal the quantitative differences in activation patterns. The comparison of the <72h and 1 month data of the mTBI group presented elevated BOLD signal at <72h in a circumscribed area of the medial prefrontal cortex and in a subtle part of the posterior cingulate gyrus. As in the hometown walking task, the cross sectional comparison yielded no significant results, thus we relied on the longitudinal data and expected the <72h state as more altered supposing a recovery over time.

Considering the BOLD signal reduction seen in our study during the <72h hometown walking task, BOLD signal elevation after brain injury is also a previously observed phenomenon, and is often explained to be an effect of neural reorganization or functional accommodation[90, 94, 167].

In the present case the additional BOLD signal during word generation task after injury was seen in the medial prefrontal cortex that is not known to be included in the language generation, instead is regarded to be part of the default mode network[150, 168] , which involves brain areas that conduct functions when not concentrating on external information. On the other hand, these areas get inactive during different tasks that require concentration[169].

From this point of view, one possible cause of the additional BOLD signal apparent at <72h compared to 1 month is a reduced deactivation capability at <72h. To confirm this, we performed additionally the calculations of deactivation contrast averages at both traumatic and control

groups at both time points and compared the extents of deactivations, focusing on the medial prefrontal area. In this area, a smaller extent of deactivation at <72h compared to 1 month was evident of the covert word generation deactivation patterns of the mTBI group (presented on **Fig. 3.2.11).** Supposing a similar variance of BOLD signal at the two time points, this result supports that the initially observed extra BOLD signal of the mTBI group at <72h is an effect of reduced deactivation. This finding is consistent with the report of Chen et al[170]. The reduced deactivation during the task is likely to represent an inability of proper redistribution of neural resources. This alteration may lead reasonably to cognitive deficits, as the impairment of default mode network was showed to correlate with different diseases, e.g. autism, schizophrenia and Alzheimer's disease [112, 168].

The presence of the few significant clusters at the longitudinal analysis of the control groups on word generation task was unexpected. The cluster located at the anterior hippocampus-parahippocampal gyrus, seen on second time point minus first time point contrast, may be an effect of the task repetition, just as the subject was inevitably remembering the words generated at the first time point –an assumption subsequently confirmed by the subjects. However, this alteration is clearly different from the one seen in the traumatic group.

In sum, the findings of reduced activation and deactivation within the same group of patients are congruent with the theory that recruitment of neural substrates is impaired in mTBI. Previous studies suggested different explanations of the altered BOLD distribution observed in mTBI, as axonal disruption, neural reorganization, functional compensation and recently, the mechanism of cognitive control[171, 172]. Based on the relatively dynamic change of cortical patterns presented in this study, the altered patterns following mTBI are rather caused by functional disarrangement

than reorganization. Our study did not confirm the role of cognitive control after injury in the absence of true additional activation areas.

To date, the exact association between mTBI related symptoms and altered cortical patterns remains controversial. Some studies presented correlation of abnormal patterns and worsened performance or ongoing symptoms[93, 103, 173]; while others found altered patterns in mTBI patients even beside normal performance[91, 96, 167]. We assume that such inconsistency may originate from the relatively large differences in actual injury severity involved in the mTBI class. Susceptibility weighted imaging, as used in this study, may be a helpful tool in assuring more homogeneous groups concerning injury severity.

The tasks performed in this study were intended to be easy to perform for mTBI patients as well, as both tasks involve essential functions. Therefore these tasks do not differentiate participants by the performance. Despite of this, the mTBI group showed significantly different fMRI findings between the two time points. This means that the altered cortical patterns are not necessarily dependent on actual performance but are a consequence of the injury per se. Other puzzling factor in the assessment of neural mechanisms behind cortical patterns is the matter of attention, as some studies have proposed[173, 174]. The potential effect of differences in attention among patients was somewhat eliminated in the hometown walking task, given that the baseline period was active counting by odd numbers instead of resting. The contrast between the two periods theoretically did not depend on the actual level of attention itself, rather on memory recall.

Overall, our results suggest a general impairment of neural flexibility after mTBI that is convalescing in the first month after the injury and tends to be independent of actual

performance or the status of attention of our patients. The reduced rate of both deactivation and activation that may lie behind the complaints in mTBI demonstrates the importance of proper capacity of metabolic recruitment, and the network –like functioning of the healthy brain.

Limitations

The main limitation of these studies were the relatively low number of subjects. This was most disadvantageous during the volumetric cross-sectional analysis which revealed no significant differences, due to great variance in volumes of cerebral structures. The need of a far greater population to perform reliable cross-sectional volumetric analysis was established in previous studies[175]. Thus, the exact direction of volume changes detected in the TBI group remained undetermined.

A weakness of DTI, resulting from its technical nature is the unpredictable effect of complex fiber architecture as fiber crossing or merging[176]. The potentially higher vulnerability of these complex fiber sites increases the importance of this problem when performing DTI studies in TBI.

For the fMRI studies, the low number of patients may be a reason why cross sectional analysis is not able to reveal significant differences between control and mTBI patients and so the exact direction of activations remains speculative. Although the tasks applied are relatively equally performable both by healthy and injured patients, thus a disturbing effect of difference in performance is not expected, the actual performance cannot be monitored in this method. The hometown walking task baseline period did also involve conscious function (counting), that is from one side advantageous as the concentration itself did not affect the fMRI contrast, while on

the other hand the absence of resting state in the paradigm complicates the interpretation and no inference can be drawn concerning the default mode network. The altered cortical patterns may be associated at a certain degree with the BOLD redistribution related to counting function as well. However, the anatomical site of detected differences in BOLD signal refers to the function that it is related to.

Originating from the nature of fMRI examination and group analysis, the projection of these results to individual level is challenging, nevertheless is required when fMRI is used to evaluate clinical correlates of a mTBI patient. For this purpose, considering the higher reproducibility of fMRI within a subject than across subjects[162, 177], the implementation of follow up investigations is suggested.

IV. QUANTITATIVE CT IN SEVERE TRAUMATIC BRAIN INJURY

4.1 Subjects and methods

Subjects

This retrospective analysis was performed on data from 84 adults with blunt sTBI (Glasgow Coma Scale≤8) requiring a ventriculostomy presenting to a Level I Trauma Center (University of Florida Trauma System, Shands Hospital in Gainesville, Florida) from 2007 to 2010. For image analyses, 76 patients were included for whom both admission and follow-up CT scans were available (eight patients without follow-up imaging were excluded from the analyses). This group of patients included 57 males and 19 females, with an average age of 40 years (SD = 15.1, min = 18, max = 75).

To test normal lateral ventricle volume asymmetry, a control group including 74 random patients from University of Florida Shands Hospital (26 patients) and the Department of Neurosurgery, University of Pécs (48 patients) without a history of moderate or sTBI nor any pathological CT alteration were added to the study (40 males, average age: 57.27 years, SD = 18.68, min = 18, max = 93).

Approval from the Institutional Review Board (IRB) of the University of Florida, and University of Pécs to conduct this study was received. Written informed consent was obtained from all participants (or legally authorized representative) in the study.

Imaging

Admission CT scans were performed within three hours in average after injury (average = 2.44, min = 1, max = 7, SD = 1.56, hours). An average of three follow-up scans within the first 10 days of sTBI were available. Routine head trauma imaging protocol was performed on Toshiba Aquilion One helical CT scanner. For the present study, standard, non-contrast head scans were used, acquired with the following parameters for both admission and follow-up scans: Slice thickness = 5 mm, axial slices, kVp = 120, mAs = 300, FOV = 512*512 pixels (227.33mm*227.33mm). Scans of same parameters were acquired in the control group.

Image analysis

Lateral Ventricle Volume measurement

Computer assisted manual volumetric measurement was conducted using Osirix™ 5.8.5 [open source] Imaging Software (http://www.osirix-viewer.com/)[178]. Left and right lateral ventricles were manually outlined in each slice using "Pencil" (freehand region of interest) tool (see **Fig. 4.1.1**). Based on the outlined areas and slice thickness information a three dimensional (3-D) reconstruction and volume estimation of the lateral ventricle was performed. Choroid plexus and intraventricular hemorrhage were included in ventricle outlines, if present.

Lateral ventricle volume ratio (LVR) calculation

Lateral ventricular asymmetry was quantified by dividing the larger lateral ventricle volume by the smaller which we term the LVR. For each sTBI patient's admission scan, the LVR was calculated. Evaluators were blinded to later patient CT scans, clinical information and outcomes.

LVR was also calculated in each control patient, to assess normal lateral ventricular asymmetry.

Inter- and intra-rater reliability of LVR measurement

Inter- and intra-rater reliability of LVR measurement was determined using Intraclass Correlation Coefficient[179]. I measured LVRs on 10 random traumatic CTs twice for intra-rater analysis, and a second rater measured them for inter-rater analysis. Two-way model, absolute agreement type was applied, both single and average measurement reliability was calculated. Analysis was run in MedCalc statistical software[180].

Midline shift assessment

Midline shift was measured as the distance between skull midline (line between anterior and posterior attachment of the falx to the skull) and the septum pellucidum at the level of the foramina of Monro. A midline shift greater than 5mm was considered significant. Midline shift was evaluated on all (admission and follow-up) scans of the sTBI patients.

Figure 4.1.1. Illustration of manual lateral ventricle outlining. Left and right lateral ventricles were separately, manually outlined based on image anatomy and contrast in each relevant slice. (Present image shows outlining of the left ventricle in one slice.) Then, using outlined areas from each slice and slice thickness information the software performed 3D reconstruction and volume calculation of each lateral ventricle separately.

Statistics

ROC analysis of LVR and midline shift development

To determine the best admission scan LVR threshold that may be associated with the development of midline shift, a Receiver Operating Characteristic (ROC) curve analysis[181, 182] was performed using LVR as variable and midline shift development as the classification variable as follows:

Negative group: patients with no significant midline shift on admission or follow-up scans. Positive group: patients with no significant midline shift on admission scan, but with significant midline shift present on any follow-up scans. Thus, patients with significant midline shift on admission scan were excluded from this test. ROC analysis was performed according to DeLong et al[183], an exact binomial confidence interval for the Area Under the Curve was calculated. ROC analysis was performed using MedCalc statistical software.

Odds ratio and relative risk test for “high LVR” and midline shift development

The LVR threshold of best sensitivity and specificity yielded by ROC analysis was then used to define “high admission LVR” and “low admission LVR” patient groups. Odds (OR) and relative risk (RR) ratios were calculated taking “high admission LVR” group as exposed group; “low admission LVR” group as control group; patients with no midline shift on admission or follow-up scans as good outcome cases, patients with no significant midline shift on admission scan, but with significant midline shift on any follow-up scans as poor outcome cases using MedCalc statistical software.

4.2 Results

The average LVR for all evaluated sTBI patients (n = 76) on admission scans was 2.03 (SD = 1.401), median was 1.51 (min. LVR = 1.01, max. LVR = 9.67). Sixteen patients had significant midline shift on admission scans while 60 did not. Of these 60 patients, 15 (25%) patients developed significant (>5mm) midline shift on follow-up scans.

In the control group (n = 74), average LVR was 1.14 (SD = 0.11), median was 1.11 (min. LVR = 1.00, max. LVR = 1.44).

Inter- and intra-rater reliability of LVV ratio measurement

Intra-rater intraclass correlation was 0.9445 for single measures (95% confidence interval = 0.8018 - 0.9858) and 0.9715 for average measures (95% confidence interval = 0.8900 - 0.9928). Inter-rater intraclass correlation was 0.9061 for single measures (95% confidence interval = 0.6840 - 0.9755) and 0.9508 for average measures (95% confidence interval = 0.8124 - 0.9876).

ROC analysis of LVR and midline shift development

Admission LVR of >1.67 was shown to have a sensitivity of 73.3% and a specificity of 73.3% for subsequent midline shift development (AUC = 0.782, standard error = 0.0659, 95% confidence interval = 0.657 to 0.878, z statistic = 4.28, Significance level p (area = 0.5) <0.0001). ROC curve is shown in **Fig 4.2.1.**

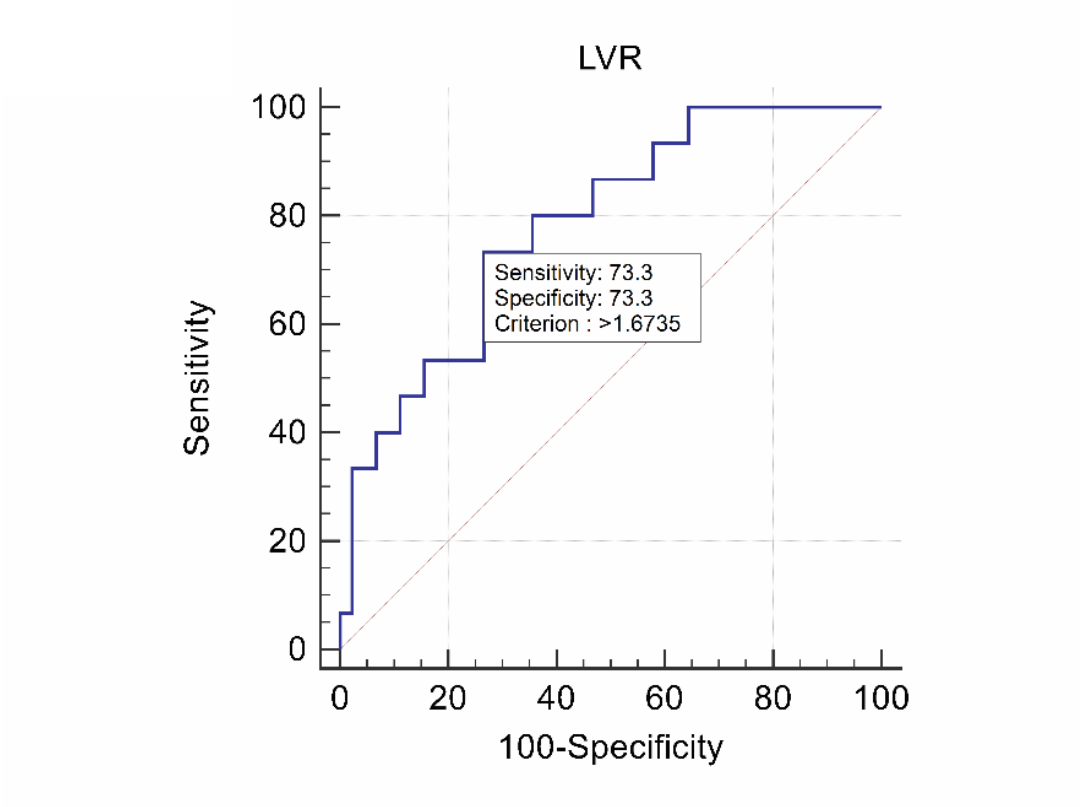

Figure 4.2.1. ROC curve analysis of Lateral Ventricle Volume Ratio (LVR) on predicting subsequent midline shift development. Only patients without significant midline shift on admission scan were included. Positive group was formed by patients who developed significant midline shift on follow-up scan, negative group was formed by patients who did not.

Odds ratio and relative risk test

When using LVR of >1.67 as criterion for "high admission LVR", 23 patients out of 60 were included in the "high admission LVR" group without significant midline shift on admission scans. Eleven of these patients (47.8%) developed midline shift on follow-up scans. In the "low admission LVR" group (n = 37), 4 patients developed midline shift on follow-up scans (10.8%).

This yielded an OR of 7.56 (95% CI = 2.0173 - 28.3502, p = 0.0027), and a RR of 4.42 (95 % CI = 1.5965 to 12.2586, p = 0.0042).

Fig. 4.2.2 shows a representative CT from the "high admission LVR" patient group with a LVR of 3.24 at admission (< 3 h post-injury) who developed midline shift on the follow-up CT scan (performed at 20 h post-injury).

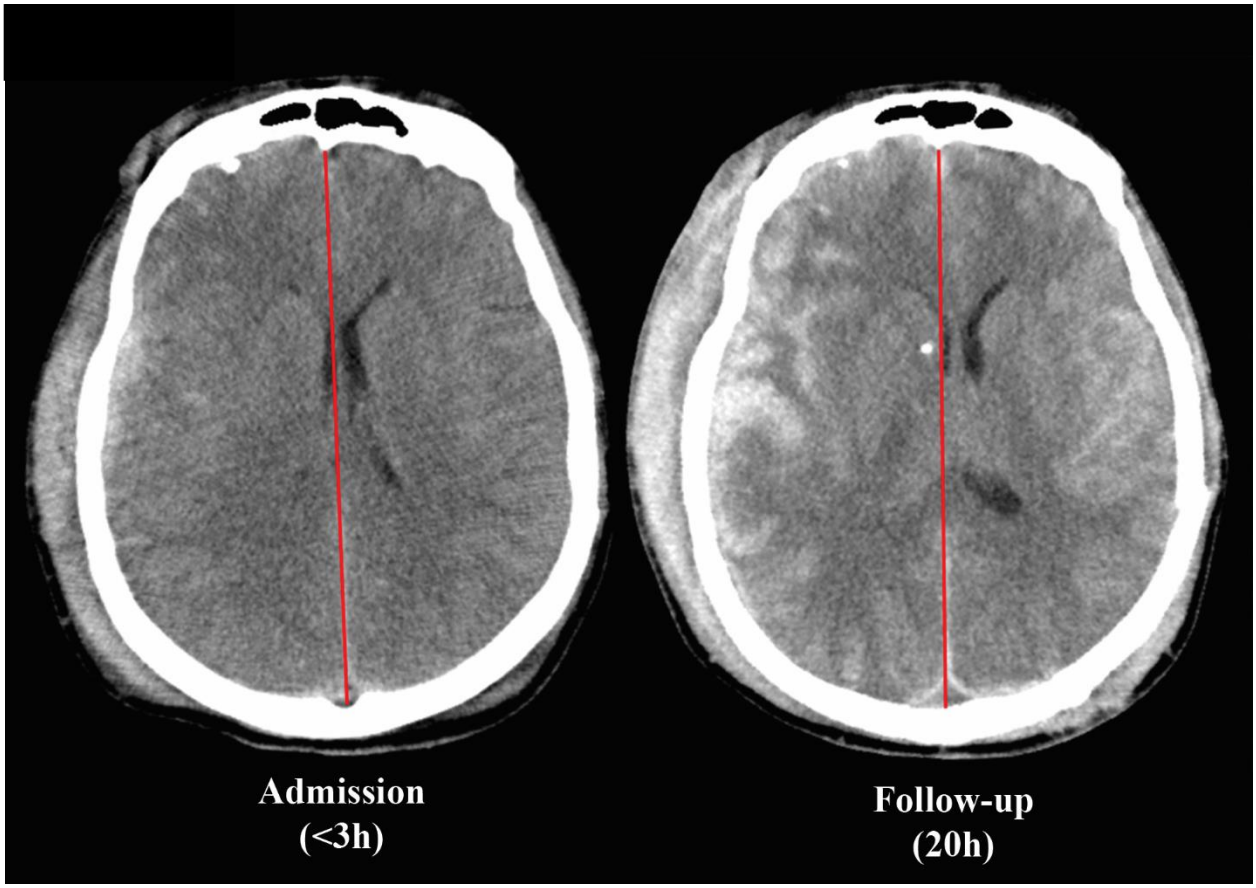

Figure 4.2.2. Admission and follow-up CT scan images of a representative patient with high admission LVR who subsequently developed significant midline shift. Midline shift was measured 1mm (not significant) on admission scan (<3 h post-injury) (**left**), while it has become 7mm (significant) on the follow-up scan at 20 h (**right**). The red line indicates the midline. External ventricular drainage is present on follow-up scan (hyperintense dot near right lateral ventricle).

4.3 Discussion

In this study, we investigated whether lateral ventricular asymmetry on admission CT scans was related to subsequent midline shift development in patients with sTBI. LVR measurement was introduced as a simple way of quantifying lateral ventricle asymmetry. In the group of patients who had no significant midline shift in their admission CT scan (< 3hr), ventricular asymmetry predicted subsequent midline shift development.

The best threshold of defining high lateral ventricular asymmetry was determined to be a LVR of >1.67, which had a 73.3% sensitivity and specificity in predicting midline shift on follow-up scans (AUC of 0.782). Patients with high LVR in admission scans had more than four-fold greater risk (RR of 4.42) to develop subsequent significant (> 5mm) midline shift than patients with low LVR. This value of "high" LVR (>1.67) was found to significantly differ from the normal (control group) LVR range (average LVR was 1.14 (SD = 0.11), median was 1.11 (min. LVR = 1.01, max. LVR = 1.44). It is possible that ventricles have a higher "compliance" for ongoing asymmetric pathologies and consequential inter-hemispherical pressure gradients than midline structures and therefore may indicate asymmetric brain pathology earlier. When unilateral hemispherical pressure is increased (by e.g. bleeding, edema), it may cause ipsilateral ventricular compression that precedes subfalcine herniation or distortion of the cerebral falx. Another possible mechanism is unilateral ventricular entrapment (foramen of Monroe blockage), where the ventricle itself causes hemispherical pressure increase and then midline shift. **Fig. 4.3.1** illustrates our concept of ventricular asymmetry predicting midline shift during asymmetric pathology development.

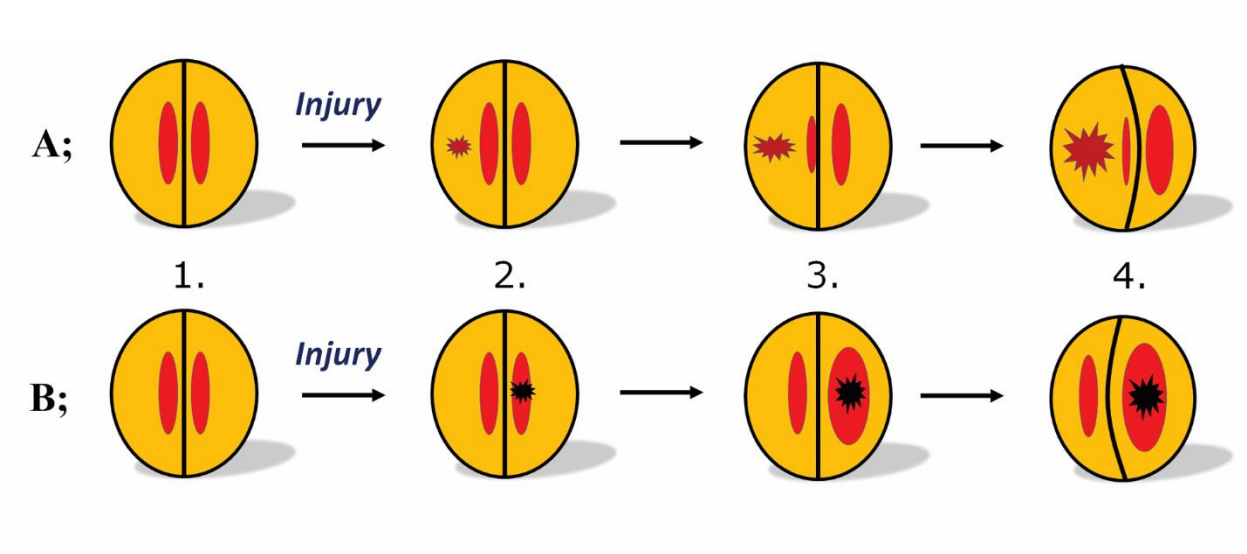

Figure 4.3.1. Concept of asymmetric intracranial pathology development.

A; 1. Normal brain 2. Initiation of asymmetric brain pathology (e.g. bleeding, edema) 3. Pathology propagation, ipsilateral ventricle compression causing lateral ventricular asymmetry 4. Further propagation causing midline shift.

B; 1. Normal brain 2. Initiation of ventricular entrapment 3. Pathology propagation, ventricle enlargement causing lateral ventricular asymmetry 4. Further propagation causing midline shift

This theory also raises that compartmental pressure elevation may predict and precede general intracranial pressure increase.

No other mass effect signs may so simply and directly indicate forthcoming midline shift. It's technically very difficult to evaluate other factors that would correctly indicate the level of inter-hemispheric pressure differences such as sulcal effacement, cisternal compression, or intracranial bleeding. Moreover, these signs often appear in combination and in both

hemispheres to a certain extent. Therefore, ventricular asymmetry may act as the “resultant CT sign” among other mass effect signs when evaluating inter-hemispheric pressure gradient.

Such an early indicator of asymmetric brain distortion may be clinically relevant and facilitate the detection of evolving intracranial pathology better than midline shift. LVR can be quickly and reliably detected on routine CT scans using open source software. For an experienced observer, the evaluation of LVV and LVR per patient took less than 5 minutes to complete. This multi-slice, 3-D reconstruction of ventricles is superior to single slice or linear ventricle measurements since 3-D measurement is less affected by image orientation and accounts for all portions (horns) of the lateral ventricles. However, in a routine clinical situation (emergency radiology) when 3D analysis may not be possible, linear measurements or subjective evaluation may still help to recognize a roughly two-fold or higher difference between lateral ventricle volumes that we propose to be predictive for midline shift. 3D analysis might be only performed in inconclusive cases.

This study has certain limitations. All patients received standard treatment for sTBI (including external ventricular drainage-EVD immediately after admission) that was modified based on type and extent of the patient’s injury. Therefore, the treatment may have prevented the development of significant midline shift in some patients with lateral ventricular asymmetry on admission CT scan. Since midline shift did not necessarily develop at the time of follow-up image acquisition, it was not possible to describe the temporal features of midline shift development and compare it to lateral ventricular asymmetry dynamics.

Future studies will be needed to investigate the value of LVR as an imaging marker in outcome prediction, compared or added to established prognostic signs and systems. However, we

propose that the main benefit of recognizing a certain level of lateral ventricular asymmetry is not outcome prediction, but the ability to detect the development of inter-hemispheric pressure gradient at a very early stage. Thus, categorization of patients into high and low risk group for development of midline shift is possible, allowing the initiation of management strategies to attenuate midline shift.

V. NOVEL FINDINGS AND CONCLUSION

Ad. Aim 1.:

Even in uncomplicated mTBI, in which by definition, conventional imaging (CT, T1w-, T2w-, FLAIR MRI) is negative, both structural and functional alterations can be detected by advanced MRI acutely after the injury:

a. High resolution volumetric analysis revealed significant brain volume changes indicative of the presence of edema in the hyperacute phase, or accelerated degenerative process in the subacute phase.

b. DTI showed a widespread diffusivity alteration in the white matter suggesting axonal disintegration acutely, which did not fully recover in a month.

c. Functional MRI has shown that both activation and deactivation rate might be reduced in the acute phase that is indicative of an overall reduced flexibility in the brain blood flow redistribution.

d. SWI allows the dichotomization of DAI into hemorrhagic and non-hemorrhagic forms based on the presence of microbleeds. Uncomplicated mTBI was associated with non-hemorrhagic DAI in our studies.

Though the majority of these alterations appeared to recover over time, a portion of them still exists over a month, in the sub-acute phase. These findings suggest that organic pathology might be just as important as the psychogenic factors in the development of the persistent post-

traumatic disorders. These and similar findings by other groups should induce a paradigm shift in the understanding of mTBI. The possible long-term consequences of the mild head injuries including sports concussions should not be overlooked, a referral to these cases as “mild” appears to be an understatement. Legal regulations regarding mTBI and concussion should be re-stated since mTBI, or a significant portion of the mTBI cases do not seem to be a disease that recovers within 8 days.

MRI may become a unique tool to recognize mTBI patients with significant underlying microstructural pathologies. These patients should be selected for a timely neurorehabilitation, which is known to lead to better outcome[184, 185].

Ad aim 2.:

The three dimensional volumetric analysis allowed an objective assessment of the ventricle deformation and asymmetry that may follow sTBI due to space occupying pathologies as bleedings and edema. We have shown that lateral ventricle asymmetry is not just linked to, but generally precedes midline shift, which is known to be a prognostic factor of poor outcome and might indicate a need of surgical intervention. The recognition of ventricular asymmetry might therefore have a similar clinical significance as midline shift has, however it indicates pathologies having a mass effect earlier than midline shift itself.

VI. LIST OF PUBLICATIONS

6.1 Publications related to the thesis

1. Multi-modal magnetic resonance imaging in the acute and sub-acute phase of mild traumatic brain injury: Can we see the difference? ***Toth A,*** *Kovacs N, Perlaki G, Orsi G, Aradi M, Komaromy H, Ezer E, Bukovics P, Farkas O, Janszky J, Doczi T, Buki A, Schwarcz A.*

JOURNAL OF NEUROTRAUMA 2013 Jan 1;30(1):2-10. doi: 10.1089/neu.2012.2486 IF: 3.968

2. Lateral Ventricle Volume Asymmetry Predicts Midline Shift in Severe Traumatic Brain Injury

Tóth A*, Schmalfuss I, Heaton SC, Gabrielli A, Hannay H, Papa L, Brophy GM, Wang KK, Büki A, Schwarcz A, Hayes RL, Robertson CS, Robicsek SA.* JOURNAL OF NEUROTRAUMA 2015 Sep 1;32(17):1307-11. doi: 10.1089/neu.2014.3696. IF: 4.377

3. Magnetic Resonance Imaging Application in the Area of Mild and Acute Traumatic Brain Injury: Implications for Diagnostic Markers? ***Tóth A***. FRONTIERS IN NEUROENGINEERING. Chapter 24 in: Brain Neurotrauma: Molecular, Neuropsychological, and Rehabilitation Aspects. Boca Raton (FL): CRC Press/Taylor & Francis; 2015.

4. Minor and repetitive head injury. *Buki A, Kovacs N, Czeiter E, Schmid K, Berger RP, Kobeissy F, Italiano D, Hayes RL, Tortella FC, Mezosi E, Schwarcz A,* ***Toth A****, Nemes O, Mondello S.* ADV TECH STAND NEUROSURG. 2015;42:147-92. doi: 10.1007/978-3-319-09066-5_8.

5. Are there any gender differences in the hippocampus volume after head-size correction? A volumetric and voxel-based morphometric study. *Perlaki G, Orsi G, Plozer E, Altbacker A, Darnai G, Nagy SA, Horvath R,* ***Toth A****, Doczi T, Kovacs N, Bogner P, Schwarcz A, Janszky J.* NEUROSCI LETT. 2014 Jun 6;570:119-23. doi: 10.1016/j.neulet.2014.04.013. IF: 2.030

6. Up to date imaging in traumatic brain injury (Hungarian) ***Tóth A****, Schwarcz A, Kálmán E, Büki A, Bogner P.* MAGYAR RADIOLÓGIA 2015. 6. Évf. 1. szám

Total impact factor related to the thesis: 10.375

6.2 Abstracts that can be cited related to the thesis

1. Advanced magnetic resonance imaging in the acute and sub-acute phase of mild traumatic brain injury: Can we see the difference? ***Toth A****, Kovacs N, Perlaki G, Orsi G, Aradi M, Komaromy H, Bukovics P, Farkas O, Doczi T, Janszky J, Schwarcz A, Buki A.* JOURNAL OF NEUROTRAUMA 29:(10) pp. A41-A42. (2012) (Neurotrauma Symposium 2012, 2012.07.22-25. Phoenix, USA) IF: 4.295

2. Lateral Ventricle Volume Asymmetry is Related to Spectrin Breakdown Product (SBDP145) Levels in Severe Traumatic Brain Injury. ***Tóth A****, Schmalfuss I, Heaton SC, Gabrielli A, Hannay H, Papa L, Brophy GM, Wang KK, Büki A, Schwarcz A, Hayes RL, Robertson CS, Robicsek SA.* JOURNAL OF NEUROTRAUMA 31:A-1–A-73 (March 1, 2014) pp. A67-68. (The 11th Symposium of the International Neurotrauma Society March 19–23, 2014 Budapest, Hungary) IF: 3.714

3. Conventional vs. quantitative approach in assessing post-traumatic ventriculomegaly and its relation to 6-month outcomes in severe traumatic brain injury. ***Tóth A****, Schmalfuss I, Heaton SC, Gabrielli A, Hannay H, Papa L, Brophy GM, Wang KK, Büki A, Schwarcz A, Hayes RL, Robertson CS, Robicsek SA.* JOURNAL OF NEUROTRAUMA 31:A-1–A-73 (March 1, 2014) pp. A66-67. (The 11th Symposium of the International Neurotrauma Society March 19–23, 2014 Budapest, Hungary) IF: 3.714

4. Lateral Ventricle Volume Asymmetry Predicts Midline Shift and 6-month Outcome in Severe Traumatic Brain Injury ***Tóth A****, Schmalfuss I, Heaton SC, Gabrielli A, Hannay H, Papa L, Brophy GM, Wang KK, Büki A, Schwarcz A, Hayes RL, Robertson CS, Robicsek SA.* JOURNAL OF NEUROTRAUMA 31:A-1–A-73 (March 1, 2014) pp. A66. (The 11th Symposium of the International Neurotrauma Society March 19–23, 2014 Budapest, Hungary) IF: 3.714

5. Lateral Ventricle Volume Asymmetry Predicts Midline Shift ***Tóth A****, Schmalfuss I, Heaton SC, Gabrielli A, Hannay H, Papa L, Brophy GM, Wang KK, Büki A, Schwarcz A, Hayes RL, Robertson CS, Robicsek SA.* JOURNAL OF NEUROTRAUMA 31:A-1–A-126 (June 15, 2014) ppA2-28. (The

32nd Annual National Neurotrauma Symposium June 29–July 2, 2014 San Francisco, California, USA) IF: 3.714

6.3 Other publications

1. Cortical involvement during myotonia in myotonic dystrophy: an fMRI study. ***Toth A****, Lovadi E, Komoly S, Schwarcz A, Orsi G, Perlaki G, Bogner P, Sebok A, Kovacs N, Pal E, Janszky J.* ACTA NEUROL SCAND. 2015 Jul;132(1):65-72. doi: 10.1111/ane.12360. Epub 2015 Jan 28. IF: 2.559

2. Microbleeds may expand acutely after traumatic brain injury. ***Toth A****, Kovacs N, Tamas V, Kornyei B, Nagy M, Horvath A, Rostas T, Bogner P, Janszky J, Doczi T, Buki A, Schwarcz A.* NEUROSCI LETT. 2016 Mar 23;617:207-12. doi: 10.1016/j.neulet.2016.02.028. Epub 2016 Feb 18. IF: 2.03

3. In vivo detection of hyperacute neuronal compaction and recovery by MRI following electric trauma in rats. ***Tóth A,*** *Kátai E, Kálmán E, Bogner P, Schwarcz A, Dóczi T, Sík A, Pál J.* J MAGN RESON IMAGING. 2016 Mar 10. doi: 10.1002/jmri.25216. IF: 3.25

4. Both hemorrhagic and non-hemorrhagic traumatic MRI lesions are associated with the microstructural damage of the normal appearing white matter. ***Tóth A****, Kornyei B, Kovacs N,*

Rostas T, Buki A, Doczi T, Bogner P, Schwarcz A. BEHAV BRAIN RES. 2017 Feb 27. pii: S0166-4328(17)30324-8. doi: 10.1016/j.bbr.2017.02.039. [Epub ahead of print]

PMID: 28249729 IF:3.02

5. Quantitative MRI analysis of the brain after twenty-two years of neuromyelitis optica indicates focal tissue damage. *Aradi M, Koszegi E, Orsi G, Perlaki G, Trauninger A,* ***Toth A****, Schwarcz A, Illes Z.* EUR NEUROL. 2013;69(4):221-5. doi: 10.1159/000345799. Epub 2013 Jan 10. IF: 1.356

6. Increased diffusion in the normal appearing white matter of brain tumor patients: is this just tumor infiltration? *Horváth A, Perlaki G,* ***Tóth A****, Orsi G, Nagy S, Dóczi T, Horváth Z, Bogner P.* J NEUROONCOL. 2016 Mar;127(1):83-90. doi: 10.1007/s11060-015-2011-y. Epub 2015 Nov 27. IF: 2.754

7. Biexponential diffusion alterations in the normal-appearing white matter of glioma patients might indicate the presence of global vasogenic edema. *Horváth A, Perlaki G,* ***Tóth A****, Orsi G, Nagy S, Dóczi T, Horváth Z, Bogner P.* J MAGN RESON IMAGING. 2016 Feb 23. doi: 10.1002/jmri.25202. IF: 3.21

6.4 Other abstracts and presentations

1. Functional Magnetic Resonance Imaging Reveals Impaired Recruitment of Neural Resources in the Acute Phase after Mild Traumatic Brain Injury. ***Tóth Arnold****, Kovács Noémi, Perlaki Gábor, Orsi Gergely, Aradi Mihály, Komáromy Hedvig, Bukovics Péter, Farkas Orsolya, Dóczi Tamás, Janszky József, Büki András, Schwarcz Attila*; EANS 2012, 2012.10.24-27. Bratislava, Slovakia.

2. Imaging the minimally damaged brain ***Tóth Arnold****, Kovács Noémi, Perlaki Gábor, Orsi Gergely, Aradi Mihály, Komáromy Hedvig, Bukovics Péter, Farkas Orsolya, Dóczi Tamás, Janszky József, Büki András, Schwarcz Attila*; 6th Pannonian Symposium on Central Nervous System Injury, 2013.04.5-6., Pécs, Hungary

3. Az enyhe koponyasérülés okozta strukturális és funkcionális eltérések vizsgálata speciális mágneses rezonancia képalkotási (MRI) módszerekkel. ***Tóth Arnold****, Kovács Noémi, Perlaki Gábor, Orsi Gergely, Aradi Mihály, Komáromy Hedvig, Bukovics Péter, Farkas Orsolya, Dóczi Tamás, Janszky József, Büki András, Schwarcz Attila* Magyar Neuroradiológiai Társaság XX. Kongresszusa, 2012.11.8-10. Eger. (2012)

4. Az enyhe koponyasérülés okozta morfológiai és funkcionális eltérések vizsgálata speciális mágneses rezonancia képalkotási (MRI) módszerekkel. ***Tóth Arnold****, Kovács Noémi, Perlaki Gábor, Orsi Gergely, Aradi Mihály, Komáromy Hedvig, Bukovics Péter, Farkas Orsolya, Dóczi Tamás, Janszky József, Büki András, Schwarcz Attila* Grastyán Endre Szakkollégium IV. Nemzetközi és X. Országos Interdiszciplináris Grastyán Konferenciája, , 2012.04.12-13. Pécs. (2012)

5. Degeneratív porckorong betegségek vizsgálata kvantitatív T2 MR mérésekkel. *Juhász Ivett, Aradi Mihály, Nagy Szilvia, Papp Marianna, Perlaki Gábor, Orsi Gergely,* ***Tóth Arnold****, Nagy Gyöngyi, Bogner Péter* Magyar Neuroradiológiai Társaság 20. kongresszusa. 20th Annual Meeting of the Hungarian Society of Neuroradiology. Eger, Magyarország, 2012.11.08-2012.11.10. p. 19-20.

6. Agyi trauma hatására kialakuló „sötét sejtek" in vivo kimutatása MR képalkotással patkányban. ***Tóth Arnold****, Szijjártó Gábor, Perlaki Gábor, Nagy Szilvia, Orsi Gergely, Schwarcz Attila, Pál József* Neuroimaging Workshop Pécs, Magyarország, 2013.04.19-2013.04.20. Pécs: p. 17.

7. Nemek közti különbség a hippokampusz térfogatában? *Perlaki G, Orsi G, Nagy Sz A, Plózer E, Altbäcker A, Darnai G,* ***Tóth A****, Dóczi T, Komoly S, Bogner P, Schwarcz A, Janszky J* Neuroimaging Workshop Pécs, Magyarország, 2013.04.19-2013.04.20. Pécs: p. 16.

8. Megváltozott szöveti diffúzió gliómás betegek épnek tűnő fehérállományában. *A Horváth, Sz A Nagy, G Perlaki, G Orsi,* ***A Tóth****, T Dóczi, Zs Horváth, P Bogner.* Magyar Neuroradiológiai Társaság 22. Kongresszusa Hajdúszoboszló, Magyarország, 2014.11.06-2014.11.08. Debrecen: p. 33.

9. Microbleeds may progress acutely after traumatic brain injury ***Tóth Arnold*** 11th Hungarian-Croatian-Slovenian Radiological Symposium 2015. november 13-14 Hévíz. (2014)

10. Követéses SWI vizsgálatok koponyasérülésben: a léziók dinamikájának feltárása. ***Tóth Arnold,*** *Kovács Noémi, Környei Bálint, Perlaki Gábor, Orsi Gergely, Bogner Péter, Büki András, Schwarcz Attila* Magyar Neuroradiológiai Társaság XXII. Kongresszusa Hajdúszoboszló, 2014. november 6-8. (2014)

11. Diffusion alterations in the normal appearing white matter of glioma and meningioma patients. *Andrea Horváth, Gábor Perlaki,* ***Arnold Tóth****, Gergely Orsi, Szilvia Nagy, Tamás Dóczi, Zsolt Horváth, Péter Bogner* Neuroimaging Workshop 2015. Szeged, Magyarország, 2015.04.17-2015.04.18.p. E-kiadvány.

ACKNOWLEDGEMENTS

I feel exceptionally favored for the years spent with the scientific work in fields of neuroimaging supported by the clinical neuroscience research group at the University of Pécs Medical School. This period has taught me the basic way of scientific thinking, has brought exciting challenges and let me know many persons who represent an ideal attitude to me both in science and life.

First I would like to express my gratitude to my mentor József Janszky, who invited me to the research group with a very friendly trust, and always supported my work with his ingenious ideas.

I am especially grateful for my mentor Attila Schwarcz for guiding and managing my scientific progress by constant excellent inspiration, critical insights and by the provided financial background.

I am particularly indebted to András Büki, for introducing me to the international relations in the field of neurotrauma, encouraging my work by invitations for collaborations and for his continuous genial support.

Péter Bogner deserves a special recognition, acting as an “unofficial mentor” by his friendly, professional support and management during my studies and for providing a reliable research background by all means.

I have to express my special thanks to Tamás Dóczi for promoting my scientific career by disseminating our research findings, giving opportunities for lectures at important meetings, excellent study ideas and all the help with scientific grants.

I feel very grateful for Steven Robicsek who figured out, realized and mentored my collaboration at the University of Florida. This period was very productive, horizon widening and brought very important memories to my life.

I have to thank Firas Kobeissy for the invitations to international collaborations and publications.

Many thanks go to the research team and staff of the Diagnostic Center of Pécs for the indispensable help and technical guide, including Gábor Perlaki, Gergely Orsi, Szilvia Nagy, Andrea Horváth, Kristóf Biczó and all operators.

I'd like to give special thanks for the collaborators from the Department of Neurosurgery including Noémi Kovács, József Pál, József Nyirádi and Endre Czeiter.

I feel principally grateful for my father, Endre Kálmán, who, despite not involved in neuroimaging in particular, has always kept an eye on my work and gave me the most important, creative and problem-solving ideas in several cases.

At last but not least, I wish to thank the rest of my family as well and my wife for encouraging my work by providing a solicitude background.

REFERENCES

1. Silver JM, M.T., Yodofsky SC, eds. (2005). Textbook of Traumatic Brain Injury. Arlington, Va: American Psychiatric Publishing.

2. Teasdale, G. and Jennett, B. (1974). Assessment of coma and impaired consciousness. A practical scale. Lancet 2, 81-84.

3. Proehl, J.A. (1992). The Glasgow Coma Scale: do it and do it right. Journal of emergency nursing: JEN : official publication of the Emergency Department Nurses Association 18, 421-423.

4. Segatore, M. and Way, C. (1992). The Glasgow Coma Scale: time for change. Heart & lung : the journal of critical care 21, 548-557.

5. Centers for Disease Control and Prevention (CDC), National Center for Injury Prevention and Control. Report to Congress on mild traumatic brain injury in the United States: steps to prevent a serious public health problem. Atlanta (GA): Centers for Disease Control and Prevention; 2003.

6. Harrison-Felix, C., Whiteneck, G., Devivo, M.J., Hammond, F.M. and Jha, A. (2006). Causes of death following 1 year postinjury among individuals with traumatic brain injury. J Head Trauma Rehabil 21, 22-33.

7. Lu, J., Marmarou, A., Choi, S., Maas, A., Murray, G., Steyerberg, E.W., Impact and Abic Study Group (2005). Mortality from traumatic brain injury. Acta Neurochir Suppl 95, 281-285.

8. Langlois JA (2006). Traumatic Brain Injury in the United States: Emergency Department Visits, Hospitalizations, and Deaths: Centers for Disease Control and Prevention.

9. Czeiter E, Sandor J., Kovacs N, Ezer E, Doczi T and Buki A (2009). The "Pecs Severe Traumatic Brain Injury Database": Outcome Estimation in Case of Severe Head Injury in Hungary. In: *Front.*

Syst. Neurosci. Conference Abstract: 12th Meeting of the Hungarian Neuroscience Society.: Budapest, Hungary.

10. Adams, J.H., Doyle, D., Ford, I., Gennarelli, T.A., Graham, D.I. and McLellan, D.R. (1989). Diffuse axonal injury in head injury: definition, diagnosis and grading. Histopathology 15, 49-59.

11. Buki, A. and Povlishock, J.T. (2006). All roads lead to disconnection?--Traumatic axonal injury revisited. Acta Neurochir (Wien) 148, 181-193; discussion 193-184.

12. Povlishock, J.T. (1992). Traumatically induced axonal injury: pathogenesis and pathobiological implications. Brain Pathol 2, 1-12.

13. Johnson, V.E., Stewart, W. and Smith, D.H. (2013). Axonal pathology in traumatic brain injury. Exp Neurol 246, 35-43.

14. Haydel, M.J., Preston, C.A., Mills, T.J., Luber, S., Blaudeau, E. and DeBlieux, P.M. (2000). Indications for computed tomography in patients with minor head injury. N Engl J Med 343, 100-105.

15. Davis, T., Ings, A., National Institute of Health and Care (2015). Head injury: triage, assessment, investigation and early management of head injury in children, young people and adults (NICE guideline CG 176). Archives of disease in childhood. Education and practice edition 100, 97-100.

16. Jeret, J.S., Mandell, M., Anziska, B., Lipitz, M., Vilceus, A.P., Ware, J.A. and Zesiewicz, T.A. (1993). Clinical predictors of abnormality disclosed by computed tomography after mild head trauma. Neurosurgery 32, 9-15

17. Falimirski, M.E., Gonzalez, R., Rodriguez, A. and Wilberger, J. (2003). The need for head computed tomography in patients sustaining loss of consciousness after mild head injury. J Trauma 55, 1-6.

18. Ingebrigtsen, T., Romner, B. and Kock-Jensen, C. (2000). Scandinavian guidelines for initial management of minimal, mild, and moderate head injuries. The Scandinavian Neurotrauma Committee. J Trauma 48, 760-766.

19. Jagoda, A.S., Cantrill, S.V., Wears, R.L., Valadka, A., Gallagher, E.J., Gottesfeld, S.H., Pietrzak, M.P., Bolden, J., Bruns, J.J., Jr., Zimmerman, R, American College of Emergency Physicians (2002). Clinical policy: neuroimaging and decisionmaking in adult mild traumatic brain injury in the acute setting. Ann Emerg Med 40, 231-249.

20. Stiell, I.G., Wells, G.A., Vandemheen, K., Clement, C., Lesiuk, H., Laupacis, A., McKnight, R.D., Verbeek, R., Brison, R., Cass, D., Eisenhauer, M.E., Greenberg, G. and Worthington, J. (2001). The Canadian CT Head Rule for patients with minor head injury. Lancet 357, 1391-1396.

21. Homnick, A., Sifri, Z., Yonclas, P., Mohr, A. and Livingston, D. (2012). The temporal course of intracranial haemorrhage progression: how long is observation necessary? Injury 43, 2122-2125.

22. Lannsjo, M., Backheden, M., Johansson, U., Af Geijerstam, J.L. and Borg, J. (2013). Does head CT scan pathology predict outcome after mild traumatic brain injury? Eur J Neurol 20, 124-129.

23. Jacobs, B., Beems, T., Stulemeijer, M., van Vugt, A.B., van der Vliet, T.M., Borm, G.F. and Vos, P.E. (2010). Outcome prediction in mild traumatic brain injury: age and clinical variables are stronger predictors than CT abnormalities. J Neurotrauma 27, 655-668.

24. Zhu, G.W., Wang, F. and Liu, W.G. (2009). Classification and prediction of outcome in traumatic brain injury based on computed tomographic imaging. The Journal of international medical research 37, 983-995.

25. Marshall, L.F., Marshall, S.B., Klauber, M.R., Van Berkum Clark, M., Eisenberg, H., Jane, J.A., Luerssen, T.G., Marmarou, A. and Foulkes, M.A. (1992). The diagnosis of head injury requires a classification based on computed axial tomography. J Neurotrauma 9 Suppl 1, S287-292.

26. Lobato, R.D., Gomez, P.A., Alday, R., Rivas, J.J., Dominguez, J., Cabrera, A., Turanzas, F.S., Benitez, A. and Rivero, B. (1997). Sequential computerized tomography changes and related final outcome in severe head injury patients. Acta Neurochir (Wien) 139, 385-391.

27. Maas, A.I., Hukkelhoven, C.W., Marshall, L.F. and Steyerberg, E.W. (2005). Prediction of outcome in traumatic brain injury with computed tomographic characteristics: a comparison between the computed tomographic classification and combinations of computed tomographic predictors. Neurosurgery 57, 1173-1182

28. Nelson, D.W., Nystrom, H., MacCallum, R.M., Thornquist, B., Lilja, A., Bellander, B.M., Rudehill, A., Wanecek, M. and Weitzberg, E. (2010). Extended analysis of early computed tomography scans of traumatic brain injured patients and relations to outcome. J Neurotrauma 27, 51-64.

29. Katsnelson, M., Mackenzie, L., Frangos, S., Oddo, M., Levine, J.M., Pukenas, B., Faerber, J., Dong, C., Kofke, W.A. and le Roux, P.D. (2012). Are initial radiographic and clinical scales associated with subsequent intracranial pressure and brain oxygen levels after severe traumatic brain injury? Neurosurgery 70, 1095-1105;

30. Steyerberg, E.W., Mushkudiani, N., Perel, P., Butcher, I., Lu, J., McHugh, G.S., Murray, G.D., Marmarou, A., Roberts, I., Habbema, J.D. and Maas, A.I. (2008). Predicting outcome after traumatic brain injury: development and international validation of prognostic scores based on admission characteristics. PLoS medicine 5, e165;

31. Han, J., King, N.K., Neilson, S.J., Gandhi, M.P. and Ng, I. (2014). External validation of the CRASH and IMPACT prognostic models in severe traumatic brain injury. J Neurotrauma 31, 1146-1152.

32. van der Naalt, J., Hew, J.M., van Zomeren, A.H., Sluiter, W.J. and Minderhoud, J.M. (1999). Computed tomography and magnetic resonance imaging in mild to moderate head injury: early and late imaging related to outcome. Ann Neurol 46, 70-78.

33. Jenkins, A., Teasdale, G., Hadley, M.D., Macpherson, P. and Rowan, J.O. (1986). Brain lesions detected by magnetic resonance imaging in mild and severe head injuries. Lancet 2, 445-446.

34. Levin, H.S., Amparo, E., Eisenberg, H.M., Williams, D.H., High, W.M., Jr., McArdle, C.B. and Weiner, R.L. (1987). Magnetic resonance imaging and computerized tomography in relation to the neurobehavioral sequelae of mild and moderate head injuries. J Neurosurg 66, 706-713.

35. Schrader, H., Mickeviciene, D., Gleizniene, R., Jakstiene, S., Surkiene, D., Stovner, L.J. and Obelieniene, D. (2009). Magnetic resonance imaging after most common form of concussion. BMC Med Imaging 9, 11.

36. Hughes, D.G., Jackson, A., Mason, D.L., Berry, E., Hollis, S. and Yates, D.W. (2004). Abnormalities on magnetic resonance imaging seen acutely following mild traumatic brain injury: correlation with neuropsychological tests and delayed recovery. Neuroradiology 46, 550-558.

37. Geurts, B.H., Andriessen, T.M., Goraj, B.M. and Vos, P.E. (2012). The reliability of magnetic resonance imaging in traumatic brain injury lesion detection. Brain Inj 26, 1439-1450.

38. Ogawa, T., Sekino, H., Uzura, M., Sakamoto, T., Taguchi, Y., Yamaguchi, Y., Hayashi, T., Yamanaka, I., Oohama, N. and Imaki, S. (1992). Comparative study of magnetic resonance and CT scan imaging in cases of severe head injury. Acta neurochirurgica. Supplementum 55, 8-10.

39. Mittl, R.L., Grossman, R.I., Hiehle, J.F., Hurst, R.W., Kauder, D.R., Gennarelli, T.A. and Alburger, G.W. (1994). Prevalence of MR evidence of diffuse axonal injury in patients with mild head injury and normal head CT findings. AJNR Am J Neuroradiol 15, 1583-1589.

40. Carroll, L.J., Cassidy, J.D., Holm, L., Kraus, J. and Coronado, V.G. (2004). Methodological issues and research recommendations for mild traumatic brain injury: the WHO Collaborating Centre Task Force on Mild Traumatic Brain Injury. J Rehabil Med, 113-125.

41. Ruff, R.M., Iverson, G.L., Barth, J.T., Bush, S.S., Broshek, D.K., Policy, NAN Policy and Planning Committee (2009). Recommendations for diagnosing a mild traumatic brain injury: a National Academy of Neuropsychology education paper. Arch Clin Neuropsychol 24, 3-10.

42. Shaw, N.A. (2002). The neurophysiology of concussion. Prog Neurobiol 67, 281-344.

43. McDowell, S., Whyte, J. and D'Esposito, M. (1997). Working memory impairments in traumatic brain injury: evidence from a dual-task paradigm. Neuropsychologia 35, 1341-1353.

44. Bryant, R.A. and Harvey, A.G. (1999). Postconcussive symptoms and posttraumatic stress disorder after mild traumatic brain injury. J Nerv Ment Dis 187, 302-305.

45. Smith-Seemiller, L., Fow, N.R., Kant, R. and Franzen, M.D. (2003). Presence of post-concussion syndrome symptoms in patients with chronic pain vs mild traumatic brain injury. Brain Inj 17, 199-206.

46. Erlanger, D.M. (2015). Exposure to sub-concussive head injury in boxing and other sports. Brain Inj 29, 171-174.

47. Belanger, H.G. and Vanderploeg, R.D. (2005). The neuropsychological impact of sports-related concussion: a meta-analysis. J Int Neuropsychol Soc 11, 345-357.

48. Wright, J.M. (2014). Medical treatment of concussion. Seminars in speech and language 35, 155-158.

49. Bigler, E.D. (2004). Neuropsychological results and neuropathological findings at autopsy in a case of mild traumatic brain injury. J Int Neuropsychol Soc 10, 794-806.

50. Bigler, E.D. and Maxwell, W.L. (2012). Neuropathology of mild traumatic brain injury: relationship to neuroimaging findings. Brain Imaging Behav 6, 108-136.

51. Pierpaoli, C., Jezzard, P., Basser, P.J., Barnett, A. and Di Chiro, G. (1996). Diffusion tensor MR imaging of the human brain. Radiology 201, 637-648.

52. Beaulieu, C. (2002). The basis of anisotropic water diffusion in the nervous system - a technical review. NMR Biomed 15, 435-455.

53. Peled, S. (2007). New perspectives on the sources of white matter DTI signal. IEEE Trans Med Imaging 26, 1448-1455.

54. Hulkower, M.B., Poliak, D.B., Rosenbaum, S.B., Zimmerman, M.E. and Lipton, M.L. (2013). A decade of DTI in traumatic brain injury: 10 years and 100 articles later. AJNR Am J Neuroradiol 34, 2064-2074.

55. Arfanakis, K., Haughton, V.M., Carew, J.D., Rogers, B.P., Dempsey, R.J. and Meyerand, M.E. (2002). Diffusion tensor MR imaging in diffuse axonal injury. AJNR Am J Neuroradiol 23, 794-802.

56. Mayer, A.R., Ling, J., Mannell, M.V., Gasparovic, C., Phillips, J.P., Doezema, D., Reichard, R. and Yeo, R.A. (2010). A prospective diffusion tensor imaging study in mild traumatic brain injury. Neurology 74, 643-650.

57. Rutgers, D.R., Fillard, P., Paradot, G., Tadie, M., Lasjaunias, P. and Ducreux, D. (2008). Diffusion tensor imaging characteristics of the corpus callosum in mild, moderate, and severe traumatic brain injury. AJNR Am J Neuroradiol 29, 1730-1735.

58. Bendlin, B.B., Ries, M.L., Lazar, M., Alexander, A.L., Dempsey, R.J., Rowley, H.A., Sherman, J.E. and Johnson, S.C. (2008). Longitudinal changes in patients with traumatic brain injury assessed with diffusion-tensor and volumetric imaging. Neuroimage 42, 503-514.

59. McKenna, M.C. (2007). The glutamate-glutamine cycle is not stoichiometric: fates of glutamate in brain. J Neurosci Res 85, 3347-3358.

60. Niogi, S.N., Mukherjee, P., Ghajar, J., Johnson, C., Kolster, R.A., Sarkar, R., Lee, H., Meeker, M., Zimmerman, R.D., Manley, G.T. and McCandliss, B.D. (2008). Extent of microstructural white matter injury in postconcussive syndrome correlates with impaired cognitive reaction time: a 3T diffusion tensor imaging study of mild traumatic brain injury. AJNR Am J Neuroradiol 29, 967-973.

61. Miles, L., Grossman, R.I., Johnson, G., Babb, J.S., Diller, L. and Inglese, M. (2008). Short-term DTI predictors of cognitive dysfunction in mild traumatic brain injury. Brain Inj 22, 115-122.

62. Messe, A., Caplain, S., Paradot, G., Garrigue, D., Mineo, J.F., Soto Ares, G., Ducreux, D., Vignaud, F., Rozec, G., Desal, H., Pelegrini-Issac, M., Montreuil, M., Benali, H. and Lehericy, S. (2011). Diffusion tensor imaging and white matter lesions at the subacute stage in mild traumatic brain injury with persistent neurobehavioral impairment. Hum Brain Mapp 32, 999-1011.

63. Sidaros, A., Engberg, A.W., Sidaros, K., Liptrot, M.G., Herning, M., Petersen, P., Paulson, O.B., Jernigan, T.L. and Rostrup, E. (2008). Diffusion tensor imaging during recovery from severe traumatic brain injury and relation to clinical outcome: a longitudinal study. Brain 131, 559-572.

64. Irimia, A., Chambers, M.C., Torgerson, C.M. and Horn, J.D. (2012). Circular representation of human cortical networks for subject and population-level connectomic visualization. Neuroimage 60, 1340-1351.

65. Wilde, E.A., Hunter, J.V., Newsome, M.R., Scheibel, R.S., Bigler, E.D., Johnson, J.L., Fearing, M.A., Cleavinger, H.B., Li, X., Swank, P.R., Pedroza, C., Roberson, G.S., Bachevalier, J. and Levin, H.S. (2005). Frontal and temporal morphometric findings on MRI in children after moderate to severe traumatic brain injury. J Neurotrauma 22, 333-344.

66. Fearing, M.A., Bigler, E.D., Wilde, E.A., Johnson, J.L., Hunter, J.V., Xiaoqi, L., Hanten, G. and Levin, H.S. (2008). Morphometric MRI findings in the thalamus and brainstem in children after moderate to severe traumatic brain injury. J Child Neurol 23, 729-737.

67. Kim, J., Avants, B., Patel, S., Whyte, J., Coslett, B.H., Pluta, J., Detre, J.A. and Gee, J.C. (2008). Structural consequences of diffuse traumatic brain injury: a large deformation tensor-based morphometry study. Neuroimage 39, 1014-1026.

68. Haacke, E.M., Mittal, S., Wu, Z., Neelavalli, J. and Cheng, Y.C. (2009). Susceptibility-weighted imaging: technical aspects and clinical applications, part 1. AJNR Am J Neuroradiol 30, 19-30.

69. Babikian, T., Freier, M.C., Tong, K.A., Nickerson, J.P., Wall, C.J., Holshouser, B.A., Burley, T., Riggs, M.L. and Ashwal, S. (2005). Susceptibility weighted imaging: neuropsychologic outcome and pediatric head injury. Pediatr Neurol 33, 184-194.

70. Tong, K.A., Ashwal, S., Obenaus, A., Nickerson, J.P., Kido, D. and Haacke, E.M. (2008). Susceptibility-weighted MR imaging: a review of clinical applications in children. AJNR Am J Neuroradiol 29, 9-17.

71. Sidaros, A., Skimminge, A., Liptrot, M.G., Sidaros, K., Engberg, A.W., Herning, M., Paulson, O.B., Jernigan, T.L. and Rostrup, E. (2009). Long-term global and regional brain volume changes following severe traumatic brain injury: a longitudinal study with clinical correlates. Neuroimage 44, 1-8.

72. Corbo, V., Clement, M.H., Armony, J.L., Pruessner, J.C. and Brunet, A. (2005). Size versus shape differences: contrasting voxel-based and volumetric analyses of the anterior cingulate cortex in individuals with acute posttraumatic stress disorder. Biol Psychiatry 58, 119-124.

73. Akiyama, Y., Miyata, K., Harada, K., Minamida, Y., Nonaka, T., Koyanagi, I., Asai, Y. and Houkin, K. (2009). Susceptibility-weighted magnetic resonance imaging for the detection of cerebral microhemorrhage in patients with traumatic brain injury. Neurol Med Chir (Tokyo) 49, 97-99; discussion 99.

74. Hasiloglu, Z.I., Albayram, S., Selcuk, H., Ceyhan, E., Delil, S., Arkan, B. and Baskoy, L. (2011). Cerebral microhemorrhages detected by susceptibility-weighted imaging in amateur boxers. AJNR Am J Neuroradiol 32, 99-102.

75. Yeo, R.A., Gasparovic, C., Merideth, F., Ruhl, D., Doezema, D. and Mayer, A.R. (2011). A longitudinal proton magnetic resonance spectroscopy study of mild traumatic brain injury. J Neurotrauma 28, 1-11.

76. Di Ieva, A., Lam, T., Alcaide-Leon, P., Bharatha, A., Montanera, W. and Cusimano, M.D. (2015). Magnetic resonance susceptibility weighted imaging in neurosurgery: current applications and future perspectives. J Neurosurg, 1-13.

77. Bigler, E.D., Blatter, D.D., Anderson, C.V., Johnson, S.C., Gale, S.D., Hopkins, R.O. and Burnett, B. (1997). Hippocampal volume in normal aging and traumatic brain injury. AJNR Am J Neuroradiol 18, 11-23.

78. Levine, B., Kovacevic, N., Nica, E.I., Cheung, G., Gao, F., Schwartz, M.L. and Black, S.E. (2008). The Toronto traumatic brain injury study: injury severity and quantified MRI. Neurology 70, 771-778.

79. Bigler, E.D., Anderson, C.V. and Blatter, D.D. (2002). Temporal lobe morphology in normal aging and traumatic brain injury. AJNR Am J Neuroradiol 23, 255-266.

80. Woodward, S.H., Kaloupek, D.G., Streeter, C.C., Kimble, M.O., Reiss, A.L., Eliez, S., Wald, L.L., Renshaw, P.F., Frederick, B.B., Lane, B., Sheikh, J.I., Stegman, W.K., Kutter, C.J., Stewart, L.P., Prestel, R.S. and Arsenault, N.J. (2007). Brain, skull, and cerebrospinal fluid volumes in adult posttraumatic stress disorder. J Trauma Stress 20, 763-774.

81. Villarreal, G., Hamilton, D.A., Graham, D.P., Driscoll, I., Qualls, C., Petropoulos, H. and Brooks, W.M. (2004). Reduced area of the corpus callosum in posttraumatic stress disorder. Psychiatry Res 131, 227-235.

82. Kitayama, N., Quinn, S. and Bremner, J.D. (2006). Smaller volume of anterior cingulate cortex in abuse-related posttraumatic stress disorder. J Affect Disord 90, 171-174.

83. Villarreal, G., Hamilton, D.A., Petropoulos, H., Driscoll, I., Rowland, L.M., Griego, J.A., Kodituwakku, P.W., Hart, B.L., Escalona, R. and Brooks, W.M. (2002). Reduced hippocampal

volume and total white matter volume in posttraumatic stress disorder. Biol Psychiatry 52, 119-125.

84. Tarnavsky, O., Segev, Y., Reider-Groswasser, I., Ommaya, A.K. and Salazar, A.M. (1996). Frontal lobe changes after severe diffuse closed head injury in children: a volumetric study of magnetic resonance imaging. Neurosurgery 38, 851.

85. MacKenzie, J.D., Siddiqi, F., Babb, J.S., Bagley, L.J., Mannon, L.J., Sinson, G.P. and Grossman, R.I. (2002). Brain atrophy in mild or moderate traumatic brain injury: a longitudinal quantitative analysis. AJNR Am J Neuroradiol 23, 1509-1515.

86. Berryhill, P., Lilly, M.A., Levin, H.S., Hillman, G.R., Mendelsohn, D., Brunder, D.G., Fletcher, J.M., Kufera, J., Kent, T.A., Yeakley, J. and et al. (1995). Frontal lobe changes after severe diffuse closed head injury in children: a volumetric study of magnetic resonance imaging. Neurosurgery 37, 392-399;

87. Cohen, B.A., Inglese, M., Rusinek, H., Babb, J.S., Grossman, R.I. and Gonen, O. (2007). Proton MR spectroscopy and MRI-volumetry in mild traumatic brain injury. AJNR Am J Neuroradiol 28, 907-913.

88. Nair, D.G. (2005). About being BOLD. Brain Res Brain Res Rev 50, 229-243.

89. Moonen, C.T., Bandettini, P., (2000). Functional MRI. Springer, Verlag: Berlin, Germany.

90. McAllister, T.W., Saykin, A.J., Flashman, L.A., Sparling, M.B., Johnson, S.C., Guerin, S.J., Mamourian, A.C., Weaver, J.B. and Yanofsky, N. (1999). Brain activation during working memory 1 month after mild traumatic brain injury: a functional MRI study. Neurology 53, 1300-1308.

91. McAllister, T.W., Sparling, M.B., Flashman, L.A., Guerin, S.J., Mamourian, A.C. and Saykin, A.J. (2001). Differential working memory load effects after mild traumatic brain injury. Neuroimage 14, 1004-1012.

92. Perlstein, W.M., Cole, M.A., Demery, J.A., Seignourel, P.J., Dixit, N.K., Larson, M.J. and Briggs, R.W. (2004). Parametric manipulation of working memory load in traumatic brain injury: behavioral and neural correlates. J Int Neuropsychol Soc 10, 724-741.

93. Chen, J.K., Johnston, K.M., Frey, S., Petrides, M., Worsley, K. and Ptito, A. (2004). Functional abnormalities in symptomatic concussed athletes: an fMRI study. Neuroimage 22, 68-82.

94. Smits, M., Dippel, D.W., Houston, G.C., Wielopolski, P.A., Koudstaal, P.J., Hunink, M.G. and van der Lugt, A. (2009). Postconcussion syndrome after minor head injury: brain activation of working memory and attention. Hum Brain Mapp 30, 2789-2803.

95. Pardini, J.E., Pardini, D.A., Becker, J.T., Dunfee, K.L., Eddy, W.F., Lovell, M.R. and Welling, J.S. (2010). Postconcussive symptoms are associated with compensatory cortical recruitment during a working memory task. Neurosurgery 67, 1020-1027; discussion 1027-1028.

96. Slobounov, S.M., Zhang, K., Pennell, D., Ray, W., Johnson, B. and Sebastianelli, W. (2010). Functional abnormalities in normally appearing athletes following mild traumatic brain injury: a functional MRI study. Exp Brain Res 202, 341-354.

97. Russell, K.C., Arenth, P.M., Scanlon, J.M., Kessler, L.J. and Ricker, J.H. (2011). A functional magnetic resonance imaging investigation of episodic memory after traumatic brain injury. J Clin Exp Neuropsychol 33, 538-547.

98. Stulemeijer, M., Vos, P.E., van der Werf, S., van Dijk, G., Rijpkema, M. and Fernandez, G. (2010). How mild traumatic brain injury may affect declarative memory performance in the post-acute stage. J Neurotrauma 27, 1585-1595.

99. Lovell, M.R., Pardini, J.E., Welling, J., Collins, M.W., Bakal, J., Lazar, N., Roush, R., Eddy, W.F. and Becker, J.T. (2007). Functional brain abnormalities are related to clinical recovery and time to return-to-play in athletes. Neurosurgery 61, 352-359; discussion 359-360.

100. Gosselin, N., Bottari, C., Chen, J.K., Petrides, M., Tinawi, S., de Guise, E. and Ptito, A. (2011). Electrophysiology and functional MRI in post-acute mild traumatic brain injury. J Neurotrauma 28, 329-341.

101. Beckmann, C.F., DeLuca, M., Devlin, J.T. and Smith, S.M. (2005). Investigations into resting-state connectivity using independent component analysis. Philos Trans R Soc Lond B Biol Sci 360, 1001-1013.

102. Sharp, D.J., Beckmann, C.F., Greenwood, R., Kinnunen, K.M., Bonnelle, V., De Boissezon, X., Powell, J.H., Counsell, S.J., Patel, M.C. and Leech, R. (2011). Default mode network functional and structural connectivity after traumatic brain injury. Brain 134, 2233-2247.

103. Chen, J.K., Johnston, K.M., Petrides, M. and Ptito, A. (2008). Recovery from mild head injury in sports: evidence from serial functional magnetic resonance imaging studies in male athletes. Clin J Sport Med 18, 241-247.

104. Mayer, A.R., Mannell, M.V., Ling, J., Gasparovic, C. and Yeo, R.A. (2011). Functional connectivity in mild traumatic brain injury. Hum Brain Mapp 32, 1825-1835.

105. Slobounov, S.M., Gay, M., Zhang, K., Johnson, B., Pennell, D., Sebastianelli, W., Horovitz, S. and Hallett, M. (2011). Alteration of brain functional network at rest and in response to YMCA physical stress test in concussed athletes: RsFMRI study. Neuroimage 55, 1716-1727.

106. Tang, L., Ge, Y., Sodickson, D.K., Miles, L., Zhou, Y., Reaume, J. and Grossman, R.I. (2011). Thalamic resting-state functional networks: disruption in patients with mild traumatic brain injury. Radiology 260, 831-840.

107. Johnson, B., Zhang, K., Gay, M., Horovitz, S., Hallett, M., Sebastianelli, W. and Slobounov, S. (2012). Alteration of brain default network in subacute phase of injury in concussed individuals: resting-state fMRI study. Neuroimage 59, 511-518.

108. Sharp, D.J. and Ham, T.E. (2011). Investigating white matter injury after mild traumatic brain injury. Curr Opin Neurol 24, 558-563.

109. Jacobs, B., Beems, T., van der Vliet, T.M., Borm, G.F. and Vos, P.E. (2010). The status of the fourth ventricle and ambient cisterns predict outcome in moderate and severe traumatic brain injury. J Neurotrauma 27, 331-340.

110. Yadav, K., Sarioglu, E., Choi, H.A., Cartwright, W.B.t., Hinds, P.S. and Chamberlain, J.M. (2016). Automated Outcome Classification of Computed Tomography Imaging Reports for Pediatric Traumatic Brain Injury. Academic emergency medicine : official journal of the Society for Academic Emergency Medicine 23, 171-178.

111. Yuh, E.L., Cooper, S.R., Ferguson, A.R. and Manley, G.T. (2012). Quantitative CT improves outcome prediction in acute traumatic brain injury. J Neurotrauma 29, 735-746.

112. Williams, D.H., Levin, H.S. and Eisenberg, H.M. (1990). Mild head injury classification. Neurosurgery 27, 422-428.

113. Levin, H.S., Grossmann R.G. (1979). The Galveston Orientation and Amnesia Test. A practical scale to assess cognition after head injury. J Nerv Ment Dis Nov; 167(11):675-84.

114. Barrick, T.R., Lawes, I.N., Mackay, C.E. and Clark, C.A. (2007). White matter pathway asymmetry underlies functional lateralization. Cereb Cortex 17, 591-598.

115. Roland, P.E., Eriksson, L., Stone-Elander, S. and Widen, L. (1987). Does mental activity change the oxidative metabolism of the brain? J Neurosci 7, 2373-2389.

116. Jokeit, H., Okujava, M. and Woermann, F.G. (2001). Memory fMRI lateralizes temporal lobe epilepsy. Neurology 57, 1786-1793.

117. van der Naalt, J., van Zomeren, A.H., Sluiter, W.J. and Minderhoud, J.M. (1999). One year outcome in mild to moderate head injury: the predictive value of acute injury characteristics related to complaints and return to work. J Neurol Neurosurg Psychiatry 66, 207-213.

118. Woermann, F.G., Jokeit, H., Luerding, R., Freitag, H., Schulz, R., Guertler, S., Okujava, M., Wolf, P., Tuxhorn, I. and Ebner, A. (2003). Language lateralization by Wada test and fMRI in 100 patients with epilepsy. Neurology 61, 699-701.

119. Schwarcz, A., Auer, T., Janszky, J., Doczi, T., Merboldt, K.D. and Frahm, J. (2008). TTC post-processing is beneficial for functional MRI at low magnetic field: a comparative study at 1 T and 3 T. Eur Radiol 18, 2594-2600.

120. Smith, S.M., Jenkinson, M., Woolrich, M.W., Beckmann, C.F., Behrens, T.E., Johansen-Berg, H., Bannister, P.R., De Luca, M., Drobnjak, I., Flitney, D.E., Niazy, R.K., Saunders, J., Vickers, J., Zhang, Y., De Stefano, N., Brady, J.M. and Matthews, P.M. (2004). Advances in functional and structural MR image analysis and implementation as FSL. Neuroimage 23 Suppl 1, S208-219.

121. Smith, S.M., Zhang, Y., Jenkinson, M., Chen, J., Matthews, P.M., Federico, A. and De Stefano, N. (2002). Accurate, robust, and automated longitudinal and cross-sectional brain change analysis. Neuroimage 17, 479-489.

122. Basser, P.J., Mattiello, J. and LeBihan, D. (1994). Estimation of the effective self-diffusion tensor from the NMR spin echo. J Magn Reson B 103, 247-254.

123. Smith, S.M., Jenkinson, M., Johansen-Berg, H., Rueckert, D., Nichols, T.E., Mackay, C.E., Watkins, K.E., Ciccarelli, O., Cader, M.Z., Matthews, P.M. and Behrens, T.E. (2006). Tract-based spatial statistics: voxelwise analysis of multi-subject diffusion data. Neuroimage 31, 1487-1505.

124. Bullmore, E.T., Suckling, J., Overmeyer, S., Rabe-Hesketh, S., Taylor, E. and Brammer, M.J. (1999). Global, voxel, and cluster tests, by theory and permutation, for a difference between two groups of structural MR images of the brain. IEEE Trans Med Imaging 18, 32-42.

125. Dale, A.M., Fischl, B. and Sereno, M.I. (1999). Cortical surface-based analysis. I. Segmentation and surface reconstruction. Neuroimage 9, 179-194.

126. Fischl, B. and Dale, A.M. (2000). Measuring the thickness of the human cerebral cortex from magnetic resonance images. Proc Natl Acad Sci U S A 97, 11050-11055.

127. Fischl, B., Salat, D.H., Busa, E., Albert, M., Dieterich, M., Haselgrove, C., van der Kouwe, A., Killiany, R., Kennedy, D., Klaveness, S., Montillo, A., Makris, N., Rosen, B. and Dale, A.M. (2002). Whole brain segmentation: automated labeling of neuroanatomical structures in the human brain. Neuron 33, 341-355.

128. Fischl, B., Salat, D.H., van der Kouwe, A.J., Makris, N., Segonne, F., Quinn, B.T. and Dale, A.M. (2004). Sequence-independent segmentation of magnetic resonance images. Neuroimage 23 Suppl 1, S69-84.

129. Fischl, B., Sereno, M.I. and Dale, A.M. (1999). Cortical surface-based analysis. II: Inflation, flattening, and a surface-based coordinate system. Neuroimage 9, 195-207.

130. Han, X., Jovicich, J., Salat, D., van der Kouwe, A., Quinn, B., Czanner, S., Busa, E., Pacheco, J., Albert, M., Killiany, R., Maguire, P., Rosas, D., Makris, N., Dale, A., Dickerson, B. and Fischl, B. (2006). Reliability of MRI-derived measurements of human cerebral cortical thickness: the effects of field strength, scanner upgrade and manufacturer. Neuroimage 32, 180-194.

131. Segonne, F., Dale, A.M., Busa, E., Glessner, M., Salat, D., Hahn, H.K. and Fischl, B. (2004). A hybrid approach to the skull stripping problem in MRI. Neuroimage 22, 1060-1075.

132. Fischl, B., van der Kouwe, A., Destrieux, C., Halgren, E., Segonne, F., Salat, D.H., Busa, E., Seidman, L.J., Goldstein, J., Kennedy, D., Caviness, V., Makris, N., Rosen, B. and Dale, A.M. (2004). Automatically parcellating the human cerebral cortex. Cereb Cortex 14, 11-22.

133. Sled, J.G., Zijdenbos, A.P. and Evans, A.C. (1998). A nonparametric method for automatic correction of intensity nonuniformity in MRI data. IEEE Trans Med Imaging 17, 87-97.

134. Fischl, B., Liu, A. and Dale, A.M. (2001). Automated manifold surgery: constructing geometrically accurate and topologically correct models of the human cerebral cortex. IEEE Trans Med Imaging 20, 70-80.

135. Segonne, F., Pacheco, J. and Fischl, B. (2007). Geometrically accurate topology-correction of cortical surfaces using nonseparating loops. IEEE Trans Med Imaging 26, 518-529.

136. Dale, A.M., Sereno, M.I., (1993). Improved localization of cortical activity by combining EEG and MEG with MRI cortical surface reconstruction: a linear approach. J Cogn Neurosci 5, 162-176.

.

137. Bartsch, A.J. De Stefano, N.; Homola, G.; Smith, S. (2004). Extending SIENA for a multi-subject statistical analysis of sample-specific cerebral edge shifts: Substantiation of early brain regeneration through abstinence from alcoholism. Tenth Int. Conf. on Functional Mapping of the Human Brain.

138. Smith, S.M. (2002). Fast robust automated brain extraction. Hum Brain Mapp 17, 143-155.

139. Jenkinson, M., Bannister, P., Brady, M. and Smith, S. (2002). Improved optimization for the robust and accurate linear registration and motion correction of brain images. Neuroimage 17, 825-841.

140. Woolrich, M.W., Ripley, B.D., Brady, M. and Smith, S.M. (2001). Temporal autocorrelation in univariate linear modeling of FMRI data. Neuroimage 14, 1370-1386.

141. Jesper L.R.A, Mark.J and Stephen.S. (2007). Non-linear optimisation. FMRIB technical report TR07JA1.

142. Jesper L.R.A. Mark.J, and Stephen.S. (2007). Non-linear registration, aka Spatial normalisation. FMRIB technical report TR07JA2.

143. Vos, P.E., Battistin, L., Birbamer, G., Gerstenbrand, F., Potapov, A., Prevec, T., Stepan Ch, A., Traubner, P., Twijnstra, A., Vecsei, L. and von Wild, K. (2002). EFNS guideline on mild traumatic brain injury: report of an EFNS task force. Eur J Neurol 9, 207-219.

144. Inglese, M., Makani, S., Johnson, G., Cohen, B.A., Silver, J.A., Gonen, O. and Grossman, R.I. (2005). Diffuse axonal injury in mild traumatic brain injury: a diffusion tensor imaging study. J Neurosurg 103, 298-303.

145. Bazarian, J.J., Zhong, J., Blyth, B., Zhu, T., Kavcic, V. and Peterson, D. (2007). Diffusion tensor imaging detects clinically important axonal damage after mild traumatic brain injury: a pilot study. J Neurotrauma 24, 1447-1459.

146. Chu, Z., Wilde, E.A., Hunter, J.V., McCauley, S.R., Bigler, E.D., Troyanskaya, M., Yallampalli, R., Chia, J.M. and Levin, H.S. (2010). Voxel-based analysis of diffusion tensor imaging in mild traumatic brain injury in adolescents. AJNR Am J Neuroradiol 31, 340-346.

147. Rosenblum, W.I. (2007). Cytotoxic edema: monitoring its magnitude and contribution to brain swelling. J Neuropathol Exp Neurol 66, 771-778.

148. Wilde, E.A., McCauley, S.R., Hunter, J.V., Bigler, E.D., Chu, Z., Wang, Z.J., Hanten, G.R., Troyanskaya, M., Yallampalli, R., Li, X., Chia, J. and Levin, H.S. (2008). Diffusion tensor imaging of acute mild traumatic brain injury in adolescents. Neurology 70, 948-955.

149. Obenaus, A., Robbins, M., Blanco, G., Galloway, N.R., Snissarenko, E., Gillard, E., Lee, S. and Curras-Collazo, M. (2007). Multi-modal magnetic resonance imaging alterations in two rat models of mild neurotrauma. J Neurotrauma 24, 1147-1160.

150. Niogi, S.N. and Mukherjee, P. (2010). Diffusion tensor imaging of mild traumatic brain injury. J Head Trauma Rehabil 25, 241-255.

151. Marmarou, A. (2007). A review of progress in understanding the pathophysiology and treatment of brain edema. Neurosurg Focus 22, E1.

152. Unterberg, A.W., Stover, J., Kress, B. and Kiening, K.L. (2004). Edema and brain trauma. Neuroscience 129, 1021-1029.

153. Heiervang, E., Behrens, T.E., Mackay, C.E., Robson, M.D. and Johansen-Berg, H. (2006). Between session reproducibility and between subject variability of diffusion MR and tractography measures. Neuroimage 33, 867-877.

154. Warner, M.A., Youn, T.S., Davis, T., Chandra, A., Marquez de la Plata, C., Moore, C., Harper, C., Madden, C.J., Spence, J., McColl, R., Devous, M., King, R.D. and Diaz-Arrastia, R. (2010). Regionally selective atrophy after traumatic axonal injury. Arch Neurol 67, 1336-1344.

155. Blatter, D.D., Bigler, E.D., Gale, S.D., Johnson, S.C., Anderson, C.V., Burnett, B.M., Ryser, D., Macnamara, S.E. and Bailey, B.J. (1997). MR-based brain and cerebrospinal fluid measurement after traumatic brain injury: correlation with neuropsychological outcome. Am J Neuroradiol 18, 1-10.

156. Henry-Feugeas, M.C., Azouvi, P., Fontaine, A., Denys, P., Bussel, B., Maaz, F., Samson, Y. and Schouman-Claeys, E. (2000). MRI analysis of brain atrophy after severe closed-head injury: relation to clinical status. Brain Inj 14, 597-604.

157. McCauley, S.R., Wilde, E.A., Merkley, T.L., Schnelle, K.P., Bigler, E.D., Hunter, J.V., Chu, Z., Vasquez, A.C. and Levin, H.S. (2010). Patterns of cortical thinning in relation to event-based prospective memory performance three months after moderate to severe traumatic brain injury in children. Dev Neuropsychol 35, 318-332.

158. Maguire, E.A., Frith, C.D., Burgess, N., Donnett, J.G. and O'Keefe, J. (1998). Knowing where things are parahippocampal involvement in encoding object locations in virtual large-scale space. J Cogn Neurosci 10, 61-76.

159. Cabeza, R. and Nyberg, L. (2000). Imaging cognition II: An empirical review of 275 PET and fMRI studies. J Cogn Neurosci 12, 1-47.

160. Maguire, E.A., Frackowiak, R.S. and Frith, C.D. (1997). Recalling routes around london: activation of the right hippocampus in taxi drivers. J Neurosci 17, 7103-7110.

161. Beisteiner, R., Drabeck, K., Foki, T., Geissler, A., Gartus, A., Lehner-Baumgartner, E. and Baumgartner, C. (2008). Does clinical memory fMRI provide a comprehensive map of medial temporal lobe structures? Exp Neurol 213, 154-162.

162. Aguirre, G.K., Zarahn, E. and D'Esposito, M. (1998). The variability of human, BOLD hemodynamic responses. Neuroimage 8, 360-369.

163. Chen, J.K., Johnston, K.M., Collie, A., McCrory, P. and Ptito, A. (2007). A validation of the post concussion symptom scale in the assessment of complex concussion using cognitive testing and functional MRI. J Neurol Neurosurg Psychiatry 78, 1231-1238.

164. Knecht, S., Drager, B., Deppe, M., Bobe, L., Lohmann, H., Floel, A., Ringelstein, E.B. and Henningsen, H. (2000). Handedness and hemispheric language dominance in healthy humans. Brain 123 Pt 12, 2512-2518.

165. Janszky, J., Mertens, M., Janszky, I., Ebner, A. and Woermann, F.G. (2006). Left-sided interictal epileptic activity induces shift of language lateralization in temporal lobe epilepsy: an fMRI study. Epilepsia 47, 921-927.

166. Tie, Y., Whalen, S., Suarez, R.O. and Golby, A.J. (2008). Group independent component analysis of language fMRI from word generation tasks. Neuroimage 42, 1214-1225.

167. Jantzen, K.J., Anderson, B., Steinberg, F.L. and Kelso, J.A. (2004). A prospective functional MR imaging study of mild traumatic brain injury in college football players. AJNR Am J Neuroradiol 25, 738-745.

168. Buckner, R.L., Andrews-Hanna, J.R. and Schacter, D.L. (2008). The brain's default network: anatomy, function, and relevance to disease. Ann N Y Acad Sci 1124, 1-38.

169. Ruff, R.M., Iverson, G.L., Barth, J.T., Bush, S.S. and Broshek, D.K. (2009). Recommendations for diagnosing a mild traumatic brain injury: a National Academy of Neuropsychology education paper. Arch Clin Neuropsychol 24, 3-10.

170. Chen, J.K., Johnston, K.M., Petrides, M. and Ptito, A. (2008). Neural substrates of symptoms of depression following concussion in male athletes with persisting postconcussion symptoms. Arch Gen Psychiatry 65, 81-89.

171. Jantzen, K.J. (2010). Functional magnetic resonance imaging of mild traumatic brain injury. J Head Trauma Rehabil 25, 256-266.

172. Hillary, F.G. (2008). Neuroimaging of working memory dysfunction and the dilemma with brain reorganization hypotheses. J Int Neuropsychol Soc 14, 526-534.

173. Mayer, A.R., Mannell, M.V., Ling, J., Elgie, R., Gasparovic, C., Phillips, J.P., Doezema, D. and Yeo, R.A. (2009). Auditory orienting and inhibition of return in mild traumatic brain injury: a FMRI study. Hum Brain Mapp 30, 4152-4166.

174. Driver, J., Blankenburg, F., Bestmann, S. and Ruff, C.C. (2010). New approaches to the study of human brain networks underlying spatial attention and related processes. Exp Brain Res 206, 153-162.

175. Steen, R.G., Hamer, R.M. and Lieberman, J.A. (2007). Measuring brain volume by MR imaging: impact of measurement precision and natural variation on sample size requirements. AJNR Am J Neuroradiol 28, 1119-1125.

176. Vos, S.B., Jones, D.K., Jeurissen, B., Viergever, M.A. and Leemans, A. (2012). The influence of complex white matter architecture on the mean diffusivity in diffusion tensor MRI of the human brain. Neuroimage 59, 2208-2216.

177. Tegeler, C., Strother, S.C., Anderson, J.R. and Kim, S.G. (1999). Reproducibility of BOLD-based functional MRI obtained at 4 T. Hum Brain Mapp 7, 267-283.

178. Colquhoun, I.R. and Burrows, E.H. (1989). The prognostic significance of the third ventricle and basal cisterns in severe closed head injury. Clinical radiology 40, 13-16.

179. Shrout, P.E. and Fleiss, J.L. (1979). Intraclass correlations: uses in assessing rater reliability. Psychological bulletin 86, 420-428.

180. Schoonjans, F., Zalata, A., Depuydt, C.E. and Comhaire, F.H. (1995). MedCalc: a new computer program for medical statistics. Computer methods and programs in biomedicine 48, 257-262.

181. Metz, C.E. (1978). Basic principles of ROC analysis. Seminars in nuclear medicine 8, 283-298.

182. Zweig, M.H. and Campbell, G. (1993). Receiver-operating characteristic (ROC) plots: a fundamental evaluation tool in clinical medicine. Clinical chemistry 39, 561-577.

183. DeLong, E.R., DeLong, D.M. and Clarke-Pearson, D.L. (1988). Comparing the areas under two or more correlated receiver operating characteristic curves: a nonparametric approach. Biometrics 44, 837-845.

184. Wade, D.T., King, N.S., Wenden, F.J., Crawford, S. and Caldwell, F.E. (1998). Routine follow up after head injury: a second randomised controlled trial. J Neurol Neurosurg Psychiatry 65, 177-

185. Ponsford, J., Willmott, C., Rothwell, A., Cameron, P., Ayton, G., Nelms, R., Curran, C. and Ng, K. (2001). Impact of early intervention on outcome after mild traumatic brain injury in children. Pediatrics 108, 1297-1303.